DYNAMICS OF AN OIL CONTAINMENT BOOM IN A WAVE FIELD

by

Samuel H. Drake

B.S., Massachusetts Institute of Technology
(1965)

SUBMITTED IN PARTIAL FULFILLMENT OF THE

REQUIREMENTS FOR THE DEGREE OF

MASTER OF SCIENCE

at the

MASSACHUSETTS INSTITUTE OF TECHNOLOGY

June, 1970

Signature of Author.....
Department of Mechanical Engineering, June 4, 1970

Certified by.....
Thesis Supervisor

Accepted by.....
Chairman, Departmental Committee on Graduate Students

ABSTRACT

DYNAMICS OF AN OIL CONTAINMENT BOOM IN A WAVE FIELD

by

Samuel H. Drake

Submitted to the Department of Mechanical Engineering on June 4, 1970 in partial fulfillment of the requirement for the degree of Master of Science.

A theoretical model was developed for the magnitude and phase of the surge or horizontal displacement of an elastically constrained flat plate boom model. An experiment was set up and data was taken in an attempt to verify the theoretical model. The resulting data supported the theoretical model within the range of the experiment.

Thesis Supervisor: David P. Hoult

Title: Associate Professor of Mechanical Engineering

ACKNOWLEDGEMENTS

The author would like to sincerely thank Professor David Hoult for his guidance and many ideas and Professor Jerome Milgram for his help with the theoretical background and making available the use of his precision wavetank. The author would also like to thank Miss Sara Rothchild for her help in preparing the manuscript and his wife, Alice, for her help in proof reading the manuscript and her acceptance of my irregular hours.

This research was sponsored by the Department of the Interior, FWPCA contract no. 15080 ESL.

TABLE OF CONTENTS

LIST OF TABLES AND ILLUSTRATIONS

TABLE OF SYMBOLS

a	boom draft
a_{X0}, a_{X1}, a_{X2}	Fourier cosine coefficients for horizontal displacement
a_{A0}, a_{A1}, a_{A2}	Fourier cosine coefficients for waveheight
A	waveheight
b_{X1}, b_{X2}	Fourier sine coefficients for horizontal displacement
b_{A1}, b_{A2}	Fourier sine coefficients for waveheight
B	damping coefficient
F_c	constraining force
F_D	damping force
F_I	inertial force
F_m	added mass force
F_x	excitation force
g	gravitation acceleration
G	as defined by Eq. 17
H	as defined by Eq. 18
i	$\sqrt{-1}$
I	moment of inertia
J	nondimensional force coefficient
K	wave number
L	length of tension members
M	mass of boom
M_a	added mass of fluid
P_D	damping coefficient

P_M	added mass coefficient
Q	as defined by Eq. 52
R	as defined by Eq. 53
S	as defined by Eq. 51
T	tension force
V	magnitude of boom velocity
x	horizontal distance
α	as defined by Eq. 15
β	as defined by Eq. 16
$\gamma\pm$	reflected wave potential coefficient
η	wave surface elevation
ζ	phase angle between surge and waveheight
ζ_A	phase angle of waveheight data
ζ_χ	phase angle of surge data
θ	phase angle between exciting force and surface elevation
λ	wavelength
ξ	displacement from centerline
ρ	density of fluid
τ	nondimensional tension coefficient
ϕ	reflected wave potential
χ	horizontal displacement coefficient
$\psi\pm$	phase angle due to $\gamma\pm$
ω	frequency of waves in radians/sec.

INTRODUCTION

In recent years there has been a large increase in the amount of oil both transported across the oceans in tanks and produced on offshore platforms. Along with this increase has come the seemingly inevitable increase in the amount of oil spilled on the oceans and bays with the attendant destruction of wildlife and the contamination of beaches. Some of these oil spills such as those caused by the practice of pumping contaminated ballast water overboard, can be easily prevented. While greater care might prevent some of the accidents, particularly those occuring during loading and unloading, it is highly probable that oil spills will continue to be a serious pollution problem.

In the past, three approaches have been taken to control oil slicks: chemical dispersants or emulsifying agents, burning, and mechanical containment. While the detergents and emulsifying agents may cause a disappearance of the physical oil slick, the oil is not removed from the oceans but rather it is only dispersed and mixed with the water or allowed to sink to the bottom. The oil must still be removed by natural decomposition. Also some of the chemicals that have been used have also proved to be harmful to the natural environment. Burning or partially burning off the oil slick is sometimes possible particularly if the slick is composed of the more volatile compounds and if the slick is not too thin. The primary problem with burning off the slick is that the heat loss thru the slick to the water is so great that the temperatures needed to sustain the combustion cannot be maintained. Recently materials have

been introduced that are designed to act as a wick for the oil and thus draw some of the oil up away from the cold water by capillary action permitting the necessary temperatures for combustion to be sustained. Even in this case it is unlikely that all of the heavier or less volatile materials will be burned. Also, there is a large amount of oily smoke produced which would be objectionable near populated coastal areas.

The best alternative might be mechanical containment and subsequent collection if it were possible, as not only would the oil be totally removed from the ocean but the economic value of oil could also be recovered. In the past, a number of different designs of both solid (although flexible) and pneumatic or inflatable oil containment booms have been tried ranging from a simple line of logs chained together to a structure made by lashing a long string of barges together. The use of air bubble curtains has also been considered although the power needed appears to be too great for any large scale use. Some of the mechanical booms have worked quite well inside harbors or other protected waters, but thus far the booms have not been satisfactory when higher winds, waves, or currents are present.

The purpose of this thesis was to study the dynamics or motion of an oil containment boom model under the influence of waves. A theoretical model is presented which predicts the magnitude of the ratio of the surge or horizontal displacement to the wave height and the phase lag between the surge displacement and the wave height for

an elastically constrained flat plate boom model aligned parallel to the incident waves. This theoretical model considers the elastic constraining force, the inertial force, the exciting force due to the incident wave and both a drag and added inertia force due to the reflected wave. As the exciting force due to the incident wave and the forces due to the reflected wave are expressed in terms of a damping coefficient and an added mass coefficient which are a functions of the nondimensional term Ka where K is the wave number and a is the boom draft, the nondimensional ratio of the surge displacement to the waveheight is presented as a function of Ka.

Experimental data on this motion were taken with a suitably scaled flat plate boom model suspended in a wave tank varying the parameter Ka over an order of magnitude range in the area of interest and varying the waveheight to the point of breaking waves. This data was then used in an attempt to experimentally justify the theoretical model. This theoretical model could then be used to predict the motion of a boom with a more complicated shape if the damping and added inertia coefficients can be experimentally determined as a function of Ka. This coupled with a knowledge of the boom behavior under conditions of wind and current should permit the designing of oil containment barriers to operate satisfactorily under open sea conditions.

THEORY

As the theoretical values for the damping and inertial coefficients for a swaying or surging (the horizontal motion of a boom being referred to as surge and the vertical motion being referred to as heave) flat plate are presently available, the model was limited to a flat plate. The forces on the boom considered by the theory were limited to the constraining forces, the inertial force, the force due to the incident wave and the forces due to the reflected wave. Only one degree of freedom was considered, that of surge. However, a similar theory would hold for heave and roll.

The boom or flat plate was constrained by an elastic member at each end such that the forces were purely tensional at zero displacement (see Figure 1). If x is the horizontal or surge displacement, the constraining force in the x direction is $-x \frac{2T(x)}{L(x)}$ where T is the tension force applied by the elastic members and L is the length of the elastic members. If $L >> x$, then the variation in length and the change in T are both small and both L and T may be considered as constants or

$$F_c = - \frac{2Tx}{L} \tag{1}$$

In order to determine the appropriate tension force, a nondimensional force coefficient, J, was defined as the ratio of the constraining force per unit length of boom to the exciting force of the incident wave. As will be shown the exciting force per unit length of boom is proportional to $\rho g A a$ where ρ is the water density,

g is the gravitational acceleration, A is the waveheight and a is the boom draft. Therefore the nondimensional term, J, for the two dimensional flat plate model parallel to the incident waves is

$$J = \frac{2Tx}{L\ell\ \rho gAa} \tag{2}$$

where ℓ is the length of the boom.

In the full scale case, the boom cannot be considered as a rigid body and the constraining force per unit length must be found in terms of a differential displacement. It is assumed that the displacement from the relaxed position is proportional to the waveheight and is sinusoidal with the same wavelength as the incident waves or

$$\xi \sim A \sin\left(\frac{2\pi x}{\lambda}\right) \tag{3}$$

where ξ is the displacement from the relaxed position and λ is the wavelength of the incident wave. Considering a small element Δx of boom, the components of the tension force that are acting to constrain boom to its relaxed position are $\frac{\partial \xi}{\partial x}\Big|_1$ and $\frac{\partial \xi}{\partial x}\Big|_2$ where the subscripts 1 and 2 refer to the left and right end of the boom element (see Figure 2). Therefore the constraining force per unit length on this element of boom is

$$F_c = T' \frac{\left(\frac{\partial \xi}{\partial x}\Big|_2 - \frac{\partial \xi}{\partial x}\Big|_1\right)}{\Delta x} \tag{4}$$

where the use of the prime mark indicates the full scale conditions. At the limit $\Delta x \to 0$

$$F_c = T' \frac{\partial^2 \xi}{\partial x^2} \tag{5}$$

or using Eq. 3

$$F_c' \sim \frac{T'A'(2\pi)^2}{\lambda'^2} \tag{6}$$

Remembering that the displacement was proportional to the wave-height:

$$F_c' \sim \frac{T'x'(2\pi)^2}{\lambda'^2} \tag{7}$$

Therefore the ratio of the constraining force to the exciting force for the full scale case is

$$J' = \frac{T'x'(2\pi)^2}{\lambda'^2 \rho g A' a'} \tag{8}$$

Setting J and J' equal, the value T/L for the model can be found in terms of T' and λ'

$$\frac{2Tx}{L\ell\ \rho g A a} = \frac{T'x'(2\pi)^2}{\lambda'^2 \rho g A' a'} \tag{9}$$

$$\frac{T}{L} = \frac{T'(2\pi)^2 a}{2\lambda'^2 a'} \tag{10}$$

where it was assumed that the ratio x'/A' was equal to x/A.

While the force coefficient J is nondimensional, it is a function of the nondimensional ratio x/A, the horizontal displacement divided by the waveheight. As will be shown, the term x/A is in turn a function of the nondimensional term Ka. A somewhat more convenient relationship that expresses the tension force in nondimensional terms and avoids this problem is

$$\tau = \frac{J}{x/A} \tag{11}$$

or making use of Eq. 2

$$\tau = \frac{2T}{L\ell\rho g a} \tag{12}$$

The inertial force is simply

$$F_I = -\frac{md^2x}{dt^2} \tag{13}$$

where m is the mass of the boom.

If the boom is assumed to surge back and forth with a sinusoidal motion (if the motion is cyclic but not sinusoidal it can be broken down into Fourier components), the motion can be represented as $x = X \cos \omega t$ or $x = Xe^{i\omega t}$. For this motion Ursell[1] gives the generated wave elevation as

$$\eta(x,t) = \chi\ \pi\alpha\ \left|\ I_1\ (Ka)\right.$$

$$\left. + L_1(Ka)\right|\ \mathrm{Re}\ [e^{ikx + i\omega t}\ e^{-i\tan^{-1}(G/-H)}] \tag{14}$$

where

$$\alpha = 1/[\pi^2 I_1^2(Ka) + K_1(Ka)]^{1/2} \tag{15}$$

$$\beta = \frac{1}{2} - \frac{1 - Kb}{Ka}\ I_1(Ka) + L_1(Ka) \tag{16}$$

$$G = \pi^2 a I_1(Ka)\beta\alpha^2/Ka \tag{17}$$

$$H = K_1(Ka)G/\pi I_1(Ka) = \pi a\beta\alpha^2 K_1(Ka)/Ka \tag{18}$$

and I_1, K_1, L_1 are functions defined by Watson[2]. K is the wave number

$$K = 1/\lambda = \omega^2/g \tag{19}$$

and a is the depth or draft of the flat plate in the undisturbed fluid. Kotik[3] defines the dimensionless damping and added inertia coefficients $P_D(Ka)$ and $P_M(Ka)$ respectively where

$$P_D(Ka) = \frac{F_D}{M_a\omega^2\chi} \quad \text{and} \quad P_M(Ka) = \frac{F_M}{M_a\omega^2\chi} \tag{20}$$

F_D and F_M are the amplitudes of the force per unit length exerted by the plate on the fluid in phase with the velocity and the acceleration of the plate and M_a is the mass of a semicircle of fluid of radius a

$$M_a = \rho\pi a^2/2 \tag{21}$$

The coefficients are given as:

$$P_D(Ka) = \frac{2\pi\alpha^2}{(Ka)^2} \left| I_1(Ka) + L_1(Ka) \right|^2 \tag{22}$$

$$P_M(Ka) - P_M(\infty) = \frac{1}{\pi} \int_0^\infty \frac{P_D(z)\, dz}{z - Ka} \tag{23}$$

Values for P_D and P_M along with values for $-\tan^{-1}$ (G/-H) are given by Kotik as a function of Ka in tabular form (see Table 1).

Therefore, if the boom motion is given by $x = \chi e^{i\omega t}$, the damping force exerted on the boom is

$$F_D = -iP_D(Ka)M_a\omega^2 \chi e^{i\omega t} = -P_D(Ka)M_a\omega^2 \chi e^{i\omega t + i\pi/2} \tag{24}$$

and the added inertia force on the boom is

$$F_M = P_M(Ka)M_a\omega^2 \chi e^{i\omega t} = -P_M(Ka)M_a\omega^2 \chi e^{i\omega t + i\pi} \tag{25}$$

Knowing the velocity potential for waves caused by a forced oscillation of the plate in calm water, it is possible to determine the exciting force on the plate due to incident waves by using

Haskind's[4] relations. If the velocity of the plate during the forced oscillation is represented as $V\, e^{i\omega t}$, the asymptotic radiated potential for $x \to \pm \infty$ is given as

$$\phi = V\, \gamma^{\pm}\, e^{Kz - iKx + i\omega t} \tag{26}$$

where the function $\gamma^{\pm}$ is only a function of the wave number K and the boom geometry and the superscript $\pm$ refers to the case at $x \to \pm \infty$. For the case of a symmetric body $\gamma^{+} = -\gamma^{-}$. From Eq. 26 it follows that the far field surface elevation is

$$\eta(x,t) = V\, \gamma^{\pm}\, \frac{K}{i\omega}\, e^{-ikx + i\omega t} \tag{27}$$

This can also be written as

$$\eta(x,t) = V|\gamma^{\pm}|\, \frac{K}{i\omega}\, e^{ikx + i\omega t + i\psi^{\pm}} \tag{28}$$

where $\psi^{\pm}$ is the phase angle due to $\gamma^{\pm}$. Integrating the expression for the velocity of the plate to obtain the displacement,

$$x = \frac{V}{i\omega}\, e^{i\omega t} \tag{29}$$

it is seen that $\psi^{\pm}$ is the phase angle by which the surface elevation at $x \to \pm \infty$ leads the body displacement.

If the velocity potential of an incident wave is considered to be

$$\phi_o = \frac{gA}{\omega} e^{kz - ikx + i\omega t} \tag{30}$$

where A is the wave amplitude, the exciting force per unit length for a two dimensional body is given by Newman[5] as

$$F_x = \rho g A \gamma^- e^{-i\omega t} \tag{31}$$

Using the same notation as before where ψ^- is the phase shift due to γ^- the exciting force can be written as

$$F_x = \rho g A |\gamma^-| e^{-i\omega t + i\psi^-} \tag{32}$$

From the velocity potential of the incident wave the surface elevation is seen to be

$$\eta_o(x,t) = \frac{A}{i} e^{-ikx + i\omega t} = -iA e^{-ikx + i\omega t} \tag{33}$$

or

$$\eta_o(x,t) = A e^{-ikx + i\omega t - i\pi/2} \tag{34}$$

Comparing this result with the equation for the exciting force, it can be seen that the phase angle between the exciting force and the surface elevation is $\psi^- + \pi/2$. As $\gamma^- = -\gamma^+$, $\psi^+ = \psi^- - \pi$. If θ is defined as the phase angle between exciting force and the surface elevation,

$$\theta = \psi^- + \pi/2 = \psi^+ - \pi/2 \tag{35}$$

A damping coefficient, which is the force in phase with the velocity of the oscillating plate divided by the velocity, can be determined as a function of γ^- by considering the energy carried in the radiated waves. For a symmetrical, two dimensional body, this is given by Newman as

$$B = \rho\omega(\gamma^-)^2 \tag{36}$$

Therefore the damping force per unit length is

$$F_D = - B\ V\ e^{i\omega t} = \rho\omega|\gamma^-|^2\ V\ e^{i\omega t} \tag{37}$$

From Eq. 24 this damping force is seen to be

$$F_D = iP_D(Ka)\ M_a\omega^2\ \chi\ e^{i\omega t} \tag{24}$$

or as $V\ e^{i\omega t} = i\omega\ \chi\ e^{i\omega t}$

$$B = P_D(Ka)M_a\ \omega \tag{38}$$

or using Eq. 36

$$\rho\omega|\gamma^-|^2 = P_D(Ka)M_a\ \omega \tag{39}$$

$$|\gamma^-| = \frac{[P_D(Ka)M_a]^{1/2}}{\rho} \tag{40}$$

as $M_a = \frac{\rho\pi a^2}{2}$

$$|\gamma^-| = [P_D(Ka)\ \frac{\pi a^2}{2}]^{1/2} \tag{41}$$

As the surface elevation for the radiated waves was given in Eq. 14 as

$$\eta(x,t) = \chi\ \pi\alpha|I_1(Ka) + L_1(Ka)|\mathrm{Re}[e^{ikx = i\omega t - i\ \tan^{-1}\ (G/-H)}], \tag{14}$$

the phase angle between the surface elevations at $x \to \infty$ and the body motion is $-\tan^{-1}(G/-H)$. This is exactly the same angle as ψ^+, the phase angle shift due to γ^+.

Therefore the exciting force per unit length due to an incident wave with a surface elevation

$$\eta(x,t) = A\ e^{-ikx + i\omega t} \tag{42}$$

is

$$F_x = \rho g A \frac{\overline{\pi a^2 P_D(Ka)}}{2}\ e^{i\omega t + i\theta} \tag{43}$$

where θ is the phase angle of the force with respect to the surface elevation of the incident wave

$$\theta = \psi^+ - \frac{\pi}{2} = -\tan^{-1}(G/-H) - \frac{\pi}{2} \tag{44}$$

Assuming that the forces due to the incident waves and the radiated waves are linearily additive and that the incident wave is of the form $A\, e^{i\omega t}$ and the boom displacement is $\chi\, e^{i\omega t}$ where A is the wave height and χ is a complex expression containing both amplitude and phase information, the equation of motion can be written as

$$\sum F = F_x + F_D + F_M + F_C = -\frac{md^2x}{dt^2} \tag{45}$$

or substituting the expressions derived for F_X, F_C, F_M, F_C and F_I:

$$\rho g\, A\, a\ell \overline{\frac{\pi}{2} P_D(Ka)}\, e^{i\omega t + i\theta} - P_D(Ka) M_a \omega^2 \chi\, e^{i\omega t + i\pi/2}$$

$$-P_M(Ka) M_a \omega^2 \chi\, e^{i\omega t + i\pi} - \frac{2T}{L} \chi\, e^{i\omega t} = M\omega^2 \chi\, e^{i\omega t + i\pi} \tag{46}$$

where the forces that were previously expressed as forces per unit length are multiplied by the length of the boom, ℓ. For the forces due to the motion of the boom, F_D and F_M, this is accomplished by considering the apparent mass term M_a to be

$$M_a = \rho \frac{\pi}{2} a^2 \ell \tag{47}$$

Dividing all the terms of the equation of motion by $e^{i\omega t}$, combining terms and simplifying

$$\rho g A a \overline{\frac{\pi}{2} P_D(Ka)}\, e^{i\theta} + X[(M + P_M(Ka)M_a)\omega^2 - \frac{2T}{L} - i P_D(Ka)M_a\omega^2] = 0 \tag{48}$$

or

$$\frac{X}{A} = \frac{-\rho g a \ell \overline{\frac{\pi}{2} P_D(Ka)}\, e^{i\theta}}{(M + P_M(Ka)M_a)\omega^2 - \frac{2T}{L} - i P_D(Ka) M_a\omega^2} \tag{49}$$

If this is written in the form

$$\frac{X}{A} = \frac{Se^{i\theta}}{Q + iR} \tag{50}$$

where $$S = -\rho g a \ell \overline{\frac{\pi}{2} P_D(Ka)} \tag{51}$$

$$Q = [(M + P_M(Ka)M_a)\omega^2 - \frac{2T}{L}] \tag{52}$$

$$R = - P_D(Ka)M_a\omega^2 \tag{53}$$

$\frac{X}{A}$ can be expressed as

$$\frac{X}{A} = \frac{(Q^2 + R^2)^{1/2}\, e^{i \tan(-R/Q)}\, Se^{i\theta}}{Q^2 + R^2} \tag{54}$$

or

$$\frac{\chi}{A} = \frac{Se^{i\theta + i \tan^{-1}(-R/Q)}}{(Q^2 + R^2)^{1/2}} \tag{55}$$

As S, Q, R and θ are only a function of Ka, the magnitude and phase of χ are therefore a function of the nondimensional term Ka which is the desired result. With this information it is possible to predict the motion of a flat plate or any other shape if the functions $P_D(Ka)$ and $P_M(Ka)$ are known or experimentally determined.

EXPERIMENT

The experimental part of this thesis consisted of taking data on the motion of an elastically constrained flat plate boom model suspended in a wave tank. The basic design constraints were that the apparatus be designed to make use of the precision wave tank of the Naval Architecture and Marine Engineering Department and that the data would be first taken on film with 16 mm motion picture equipment and then transferred onto computer cards.

The precision wave tank is approximately three meters long with a cross sectional width and height of 30 cm and 20 cm respectively. The mean operating water depth used during the experimental runs was 15 cm. The waves are generated with a sinusoidally driven paddle that pivots from the bottom of the tank. Both the frequency and the amplitude of the oscillation are variable, the practical amplitude being limited to the case of breaking waves and the frequency range being limited by both the finite depth effects and the reflection coefficient of the wave absorbing beach for the long wave lengths and the rate at which the paddle could be driven for short wavelengths. The scaling ratio between the experimental model and the full scale conditions is largely determined by the acceptable range of wave lengths that can be generated in the wave tank.

This range was from approximately 10 cm to 100 cm with the longer wavelengths well inside the area where the wavelength as a function of the frequency must be corrected for the effect of

finite depth. The relationship of frequency to wavelength for finite depth is

$$\nu^2 = \frac{g}{\lambda 2\pi} \tanh \left(\frac{2\pi h}{\lambda}\right) \tag{56}$$

or

$$\omega^2 = \frac{g2\pi}{\lambda} \tanh \left(\frac{2\pi h}{\lambda}\right) \tag{57}$$

where ν is expressed in cycles per second and ω in radians per second. At a wavelength of 100 cm and a depth of 15 cm the finite depth correction term $\tan H(\frac{2\pi h}{\lambda})$ is approximately equal to 0.73 and does not closely approach one until a wavelength of 30 cm ($\tan H(\frac{2\pi h}{\lambda}) = 0.995$).

If the wavelength region of interest for full scale waves is approximately 3 to 30 meters and the full scale boom height or draft is approximately one meter then, keeping the nondimensional ratio of the wavelength to boom height constant, the height of the boom model should be approximately 3 cm. Assuming an effective specific gravity of the boom of 0.8, then 2.4 cm of the boom height will ride below the calm water level or a = 2.4 cm and the range of Ka for the experiment is approximately 0.15 to 1.5.

The constraining force for the boom model is found by using the nondimensional ratio of the constraining force to the exciting force, J, as expressed in equations 2 and 8

$$J = \frac{2Tx}{L\ell\ \rho gAa} \tag{2}$$

$$J' = \frac{T'x'(2\pi)^2}{\lambda'^2\ \rho gA'a'} \tag{8}$$

where, as before, the prime marks are used to indicate the full scale conditions. Equating J and J' yields the relationship given in equation (10)

$$\frac{T}{L} = \frac{\ell T(2\pi)^2\ a}{2\lambda'^2\ a'} \tag{10}$$

If typical full scale conditions are assumed to be a tension force of 5000 lb or approximately 2.5×10^9 dynes (this condition is found by considering a full scale boom to be anchored at the ends and in a current), a wavelength of 30 meters and a ratio of a/a' as 1/30, T/L should be approximately 5×10^3 dynes. The length of the elastic constraining members is somewhat arbitrary, the main limitation being that the length be much greater than boom displacement so that the constraining force remains linear with the displacement. With the expected boom displacement not to exceed 5 cm., the length L was set at 50 cm. The tension force for the model was therefore set at 2.50×10^5 dynes. This tension force was divided by two and effectively applied at one centimeter above and below the centerline of the boom in order to provide a roll constraint or restoring moment. This two centimeter separation was somewhat arbitrary although

representative of the full scale booms which have a cable at top and bottom. The separation distance could have been modified had it been necessary to change the roll resonance frequency.

It was originally considered desirable to correctly model the moment of inertia of the boom. The nondimensional parameter that governs this is the ratio of the moment of inertia per unit length of the boom about its roll axis to the moment of inertia per unit length of a semicircular cylinder of fluid of radius around its axis.

$$\Phi = \frac{I}{\pi\rho a^4/4} \tag{58}$$

where Φ is the nondimensional parameter and I is the moment of inertia per unit length to the boom. If the full scale boom is considered to be rectangular in cross section and of uniform density then the moment of inertia per unit length is

$$I' = \frac{M'h'^2}{4} \tag{59}$$

where M' is the mass per unit length and h' is the height of the boom. Therefore

$$\Phi' = \frac{M'h'^2}{\pi\rho a'^4} \tag{60}$$

Setting Φ equal to Φ'

$$\frac{I}{\pi\rho a^4/4} = \frac{M'h'^2}{\pi\rho a'^4} \tag{61}$$

$$I = \frac{M'h'^2 a^4}{4\, a'^4} \tag{62}$$

Taking as typical full scale conditions a mass per unit length, M', of 1.6×10^3 gm/cm, a boom height, h', of 100 cm, and a boom draft of 80 cm, the moment of inertia per unit length of a model boom with a draft of 2.4 cm should be 3.24 gm cm. Multiplying this by the length of the boom, 30 cm, the total moment of inertia should be approximately 100 gm cm^2.

The final boom model was a flat plate 30 centimeters long, 3 centimeters wide and 0.7 centimeters thick. The thickness is determined by the buoyancy necessary to float the boom and the supporting members such that 20% of the boom is out of the water in still conditions. In order to transmit the constraining force over the side walls of the tank and allow the boom 5 centimeters of vertical motion an elongated horseshoe shaped piece was added to each end of the boom. To shift the center of mass of the assembly below the center of buoyancy such that the boom was stable in an upright position, a counterweight mass was added to a piece of thin aluminum tubing projecting down from the outside arm of the support member on either end of the boom. (see figure 3). The boom was made of laminated balsa wood with the end support members made of a lamination of balsa wood and adhesive backed aluminum

foil. The boom and support members were painted with a thin epoxy base paint to waterproof the balsa wood. With the brass counterweights added, the total mass was 39 grams.

The amount of inertia of the actual boom model was measured by constructing a torsional pendulum using a length of fine piano wire. The torsional spring constant was calculated by measuring the period of oscillation with a body of known moment of inertia. The measured moment of inertia for the final boom model was approximately 2200 gm cm^2 or approximately 22 times too large. This large moment of inertia is largely due to the mass of the end support members and their counterweights.

The effect of the large moment of inertia was not deemed important, however, as the roll resonance occurred at a wavelength of approximately 150 cm or outside the region of interest and the surge and roll were not strongly coupled in the region of interest. An experimental test was run at a wavelength of 66 cm using two boom models, one with a moment of inertia of 5200 gm cm^2 and the other with a moment of inertia of 2200 gm cm^2. Similar results were obtained in both cases.

On one end of the boom the tension forces were applied by a pair of thin rubber strips which were held clamped 50 centimeters from the end of the boom. On the other end of the boom the tension forces were applied by a pair of lightweight nylon cords which were also clamped 50 centimeters from the end of the boom. The exact length of the nylon cords was adjustable with screws such that the boom could be centered in the wave channel. The tension

is adjusted by running the rubber strips over a ball bearing pulley and attaching a weight pan and laboratory weights and then clamping the strips when the correct tension is obtained.

A 25 centimeter long section of one wall of the wave tank was made of transparent plastic so that the motion of boom and the water could be photographed from the side perpendicular to the travel of the waves. In order to reference the position of the boom and the wave height and to provide a reference length the plastic plate was scribed with a set of lines (see figure 6). A set of pointers was attached to one of the support members of the boom so as to mark the relative position of the boom.

The boom motion was photographed using a Hycam high speed 16 mm movie camera run at approximately 100 frames per second. The primary reason for using the high speed camera and the relatively fast framing rate was to obtain a shutter speed fast enough such that the motion of the boom would not be blurred. On motion picture cameras the shutter speed is a function of the framing rate. As the camera needed approximately 10 seconds to achieve a regulated speed, the camera was run approximately 12 seconds for each data run with the last few seconds of the film being used for data. Prior to making a sequence of data runs a calibration run was made to record the exact boom position and water height under still conditions.

After processing the film, positional data was read off the individual frames using a machine that projects an image of the frame on a ground glass screen with an x and y cursor. By moving the cursors to the point to be read and pressing a button the

information is punched directly on computer cards in a form suitable for data processing. In this way the x and y postion of a reference point are marked on, along with the y position of the water surface along the left reference line, the x and y position of the top boom pointer and the x position of the bottom pointer. By marking on a reference point on each frame, it is not necessary to precisely align each of them. The number of frames of film read for each data run depended upon the wave frequency with enough frames being read for at least 1 1/2 complete wave cycles. The format for the calibration frames was the same with the addition of the x position of the right reference position in order to calculate a scaling factor. Five frames of data were read for each calibration point.

The frequency of the water waves was measured using a capacitance probe and a paper chart recorder. The probe consisted of an insulated wire sticking down into the water with the water acting as the outer conductor. The change in capacitance caused by the change in water height as the wave swept past caused a change in the frequency of an oscillating L-C circuit which is beating with a reference circuit. The beat frequency provided a measurement of the amplitude of the wave. As the information from this probe was only used to provide a measurement of the frequency or the wavelength using Eq. 57, it was not necessary to synchronize this information with the data taken on film.

The data was analyzed using a Fortran program which calculated the horizontal and vertical displacement of the center of mass of the boom plus the roll displacement and the waveheight for each

data frame. (See Appendix A for a list of the equations used). After computing the number of frames in one wave cycle, a Fourier analysis was performed on the wave height and the horizontal and vertical displacement using the IBM system 360 scientific subroutine for the Fourier analysis of a tabulated function. The wave-height and the horizontal or surge displacements were each plotted as the tabulated function (actual data) and as the function generated by using the first Fourier coefficients (i.e., $x(t) - a_0 + a_1 \cos \omega t + b_1 \sin \omega t$) and by using the first and second coefficients (i.e., $x(t) = a_0 + a_1 \cos \omega t + b_1 \sin \omega t + a_2 \cos 2\omega t + b_2 \sin 2\omega t$) using the Calcomp plotter (see figures 9 and 10). The ratio of magnitude of the horizontal displacement to the wave-height was found by using the square root of the sum of the squares of first Fourier coefficients.

$$\left|\frac{\chi}{A}\right| = \frac{\sqrt{a_{\chi 1}^2 + b_{\chi 1}^2}}{\sqrt{a_{A1}^2 + b_{A1}^2}} \tag{63}$$

The phase angle of the waveheight and the horizontal displacement was taken to be the arctangent of the first Fourier sine coefficient divided by the first Fourier cosine coefficient or

$$\zeta_a = \tan^{-1} (b_{A1}/a_{A1}) \tag{64}$$

$$\zeta_\chi = \tan^{-1} (b_{\chi 1}/a_{\chi 1}) \tag{65}$$

Therefore the phase lag between the horizontal displacement and the waveheight is

$$\zeta = \zeta_A - \zeta_\chi \tag{66}$$

Data was taken for values of Ka of approximately 0.15, 0.20, 0.30, 0.40, 0.50, 0.75 and 1.40. At each value of Ka except Ka = 1.40 several runs were taken varying the amplitude of the waveheight up to the case of nearly breaking waves. At Ka = 1.40 only one run was possible as the wave would break with the amplitude of the paddle drive set to any position other than the lowest.

RESULTS

Theoretical values for the magnitude and phase of X/A were computed for Ka from 0.05 to 5.0 making use of Eq. 55

$$\frac{X}{A} = \frac{Se^{i\theta} + i\tan^{-1}(-R/Q)}{(Q^2 + R^2)^{1/2}} \tag{55}$$

where Q, R, and S are defined by Eq. 52, 53, and 51. (See Appendix B for the computation scheme.) These values were computed for $\tau = 0$, $\tau = 0.071$, $\tau = 0.142$, and $\tau = 0.281$ where τ is the nondimensional tension parameter:

$$\tau = \frac{2T}{L\ell\ \pi ga} \tag{12}$$

The results are expressed in tabular form in Table 2 and graphically in figures 7 and 8. From figure 7 it is seen that the parameter has little effect on the magnitude of X/A for Ka greater than 1 and that the effect is not strongly pronounced until Ka is less than 0.4. The reason for this can be seen looking at Eq. 49

$$\frac{X}{A} = \frac{-\rho ga\ell\ \overline{\frac{\pi}{2} P_D\ (Ka)}\ e^{i\theta}}{[M + P_M(Ka)M_a]\ \omega^2 - \frac{2T}{L} - iP_D(Ka)M_a\omega^2} \tag{49}$$

Both the damping force term and the inertial force term are a function of ω^2 while the constraining force term is constant. Thus for small values of Ka where ω is small, the constraining force term is the dominant term in the denominator of Eq. 49. The exciting force

is not directly dependent on ω either, although the value of P_D is a function of Ka. Thus the damping forces and inertial forces dominate at large values of Ka and the ratio χ/A becomes small.

Varying the value of τ causes a small shift in the phase of χ/A with the magnitude of the shift declining with increasing Ka as can be seen from figure 8. The small oscillations in the phase curves that occur for small values of Ka with τ not equal to zero are caused by Q being less than zero when the $-\frac{2T}{L}$ term dominates

$$Q = [M + P_M(Ka)M_a]\omega^2 - \frac{2T}{L} \tag{52}$$

A total of 16 different experimental runs were made varying the ratio Ka by changing the wavelength and varying the waveheight. The results of these runs are displayed in tabular form in Table 3 and graphically in figures 11 and 12. The letter prefix to the run number is just for identification and has no other significance. The number simply refers to the pin position used on the apparatus that generates the wave. The waveheight is not a simple function of this number as it also depends on the wave frequency. The smallest value of Ka used was approximately 0.15 and the largest value available was approximately 1.4.

The experimental results seem to fit the theoretical curve for the magnitude of χ/A quite well (see figure 11) although there is some scatter. It would have been desirable to have taken data nearer the predicted peak and on the other side of the peak if this had been possible. However, this would have meant operating with waves

several meters long in a tank only 15 cm deep. Also, it would have been better to have taken a few more points in the range of Ka from 0.8 to 1.4 although the range of Ka from 0.15 to 0.5 was considered more interesting from the point of checking the theory. The results might have been better in regard to scatter if either a larger film format had been used or if a different focal length lens had been used with small amplitude waves such that the range of motion came closer to filling the entire film frame (owing more to the nature of the machine used to read the film than to the actual film resolution).

The experimental results for the phase of χ/A are certainly of the right order of magnitude, with all except one point being within 0.2 of a radian (~12°) of the theoretical value, but do not show any clear trend as the theoretical results do not have much variance in the range of Ka from 0.15 to 1.5 (see figure 12). In order to perform a better experimental test of the phase data, it would be necessary to extend the range of the experiment out to Ka equal to 5 or more to see whether the phase shifts from approximately $-\pi/2$ to $-\pi$. This was not possible, however, with the existing apparatus as the paddle was being driven at the maximum frequency to obtain a value of Ka equal to 1.4. Again, better results with regard to scatter could have been obtained with better filming.

CONCLUSIONS

The response of the boom to a sinusoidal exciting force was found to be sinusoidal. Even for the worst case with nearly breaking waves when the magnitude of the second harmonic of the wave amplitude was 25 percent of the magnitude of the first harmonic of the wave amplitude, the magnitude of the second harmonic of the response was less than 10 percent of the first harmonic of the response (the accuracy of measurement was about the same order of magnitude).

As the motion was sinusoidal, the problem is analogous to a driven harmonic oscillator with a damping term and an added mass term that are a function of the driving frequency. As can be seen from the data, the response is proportional to the wave height amplitude for constant values of Ka. Therefore a linearized theory can be used to describe the magnitude and phase of the response of the boom to the wave-induced forces. Within experimental accuracy, the data supported the detailed theoretical model presented for the magnitude and phase of the ratio of the surge of the boom to the wave height of the incident waves.

APPENDIX A

For each frame of data, the x and y position of a reference point, the wave height along a reference line, the x and y position of the top boom marker and the x position of the bottom boom marker were read. The x position of a second reference point was also read for the calibration frames. These seven points and the grid lines are illustrated in Figure 6. The first step in the data reduction is the determination of a scaling factor KCAL.

$$KCAL = \frac{XB}{XCAL2 - XCAL1} \tag{A-1}$$

where XCAL1 and XCAL2 are the measured x positions of the reference lines and XB is the known distance between them. The boom position and water height for static conditions are then found. The water height, HCAL, is given by

$$HCAL = KCAL\ (YH - YCAL) \tag{A-2}$$

where YH is the measured reference value and YCAL is the water height along the reference line. The boom roll angle SIGCAL is given by

$$SIGCAL = SIN^{-1}\ [KCAL\ \frac{(X2 - X1)}{B}] \tag{A-3}$$

where X1 and X2 are the measured x positions of top and bottom boom markers. The static x positions of the top boom marker, X1CAL, is given by

$$X1CAL = KCAL\ (X1 - XCAL1) - XA \tag{A-4}$$

where the factor XA is used to transfer the x reference position to the center grid line. The static x position of the center of the boom, XGCAL, is given by

$$XGCAL = X1CAL + A \sin (SIGCAL) - \frac{B}{2} \cos (SIGCAL) \tag{A-5}$$

where A is the distance from the tip of the pointer to the center line of the boom. The static y position of the boom is found in a similar manner.

After determining the position of the boom and the waterline for static conditions, the surge, heave and roll displacement of the boom and the wave height were found for the dynamic conditions by using the same equations and subtracting the static or calibration values. This data was then plotted as a function of the frame number if so desired.

The next step was the calculation of the wavelength from the frequency using a recursive technique to correct for the finite depth effect. The initial approximation, $XLAM_1$, the infinite depth value was

$$XLAM_1 = \frac{G}{2\pi (FREQ)^2} \tag{A-6}$$

The correction factor, CORR, for finite depth was

$$CORR = \tanh \frac{2\pi DEP}{XLAM} \tag{A-7}$$

where XLAM was the current wavelength approximation where DEP was the depth of the water. From these an err function, ERR, was generated

$$ERR = \frac{XLAM}{CORR} - XLAM_1 \tag{A-8}$$

The next approximation to the wavelength was taken to be

$$XLAM = XLAM - 0.7 \times CORR \times XLAM \tag{A-9}$$

This was repeated until the err function was less than the desired limit.

Prior to calculating the Fourier coefficients it was necessary to calculate the number of data points per cycle. This was done by counting the number of data points from the place where the wave-height first changed the sign or went thru the origin until it changed sign for the third time. The first and second Fourier coefficients were then found for the waveheight and the surge and heave displacements by making use of a subroutine from the IBM scientific subroutine package. A function was generated by using the first coefficient and by using the first and second coefficients. These two functions were plotted along with the actual data for comparison.

The final step was to calculate the magnitude and phase of X/A. The magnitude of X/A was found by dividing the square root of the sum of the squares of the first Fourier coefficients of the

surge displacement by the square root of the sum of the squares of the first Fourier coefficients of the wave height.

$$\left|\frac{X}{A}\right| = \frac{\sqrt{ACOFXG(2)^2 + BCOFXG(2)^2}}{\sqrt{ACOFH(2)^2 + BCOFH(2)^2}} \qquad \text{(A-10)}$$

where ACOFXG(2) and BCOFXG(2) are the first fourier coefficients of the surge displacement and ACOFH(2) and BCOFH(2) are the first Fourier coefficients of the wave height. The phase of X/A was found by taking the difference between the phase of surge displacement and the phase of the wave height after the phase of the wave-height was shifted an amount $\frac{2\pi(XA)}{\lambda}$ to correct for the fact that the wave height data was taken along the left grid line instead of the centerline (XA is the distance between these two lines). The phase of each was found by taking the arc tangent of the first Fourier sine coefficient divided by the first ourier cosine coefficient. For example

$$XGPHAS = \tan^{-1} \frac{BCOFXG(2)}{ACOFXG(2)}$$

where XGPHAS is the phase of the surge displacement. A listing of the program follows.

```
      DIMENSION H(300), SIG(300), XG(300), YG(300), Z(300), YO(300),
     $HR(300), FRBRD(300), ACOFH(5), BCOFH(5), ACOFXG(5), BCOFXG(5),
     $ACOFYG(5), BCOFYG(5), XGFOR(300), XGVEL(300), XGACC(300),
     $YGFOR(300), YGVEL(300), YGACC(300)
C
C     INITIAL SETUP
C
      NOP = 0
      G = 980.35
      PI = 3.14159
      DEP = 15.0
      YAC = 10.0
      YA = 10.0
      D = 2.40
      XA = 5.0
      XB = 10.0
      A = 1.30
      B = 3.0
      KCALA = 0.0
      N = 0
      HCALA = 0.0
      SIGCA = 0.0
      X1CALA = 0.0
      Y1CALA = 0.0
      READ(5,1) NMON, NDAY, NYEAR, NRUN, KAL
    1 FORMAT (5I4)
C
C     CALCULATE CALIBRATION FACTORS
C
      DO 3 I = 1, KAL
      READ(5,2) XCAL1, YCAL, YH, X1, Y1, X2, XCAL2
    2 FORMAT (7F10.9)
      XCAL = XCAL2 - XCAL1
      KCAL = XB / XCAL
      KCALA = KCALA + KCAL
      HCAL = KCAL * (YH - YCAL) - YAC
```

```
      HCALA = HCALA + HCAL
      SIGC = ARSIN (KCAL * ((X2 - X1) / B))
      SIGCA = SIGCA + SIGC
      X1CAL = KCAL * (X1 - XCAL1) - XA
      X1CALA = X1CALA + X1CAL
      Y1CAL = KCAL * (Y1 - YCAL) - YAC
      Y1CALA = Y1CALA + Y1CAL
      N = N + 1
    3 CONTINUE
      KCAL = KCALA / N
      HCAL = HCALA / N
      SIGCAL = SIGCA / N
      X1CAV = X1CALA / N
      XGCAL = X1CAV + A * COS(SIGCAL) + (B / 2) * SIN(SIGCAL)
      Y1CAV = Y1CALA / N
      YGCAL = Y1CAV + A * SIN(SIGCAL) - (B / 2) * COS(SIGCAL)
      WRITE(6,4)
    4 FORMAT ('1CALIBRATION DATA ')
      WRITE(6,5)
    5 FORMAT ('0   KCAL       HCAL      SIGCAL     XGCAL      YGCAL')
      WRITE(6,6) KCAL, HCAL, SIGCAL, XGCAL, YGCAL
    6 FORMAT (5F10.4)
C
C     SETUP FOR DATA RUNS
C
      DO 25 L = 1, NRUN
      READ(5,7) MRUN, M, FREQ
    7 FORMAT (2I4, F10.4)
      WRITE(6,8) MRUN, NMON, NDAY, NYEAR
    8 FORMAT ('1DATA RUN',I5,'  DATE:',I3,'/',I2,'/',I2)
      WRITE(6,9)
    9 FORMAT ('0 N      H         SIG        XG         YG')
C
C     DATA REDUCTION
C
      DO 12 I = 1, M
```

```
      READ(5,10) XCAL, YCAL, YH, X1, Y1, X2
   10 FORMAT (6F10.9)
      H(I) = KCAL * (YH - YCAL) - HCAL - YA
      SIG(I) = ARSIN(KCAL * ((X2 - X1) / B)) - SIGCAL
      X1CAL = KCAL * (X1 - XCAL) - XA
      XG(I) = X1CAL + A * COS(SIG(I)) + (B / 2) * SIN(SIG(I)) - XGCAL
      Y1CAL = KCAL * (Y1 - YCAL) - YA
      YG(I) = Y1CAL + A * SIN(SIG(I)) - (B / 2) * COS(SIG(I)) - YGCAL
      Z(I) = I
      YO(I) = 0
      J = I
      WRITE(6,11) J, H(I), SIG(I), XG(I), YG(I)
   11 FORMAT ('0', I3, 4F10.4)
   12 CONTINUE
C
C     PLOT REDUCED DATA (OPTIONAL, IP = 1 FOR PLOT)
C
      IF (NOP) 13, 13, 15
   13 CALL NEWPLT ('M7754','8427','WHITE ','BLACK')
      IP = 0
      IF (IP - NOP) 15, 15, 14
   14 CALL PICTUR (15.0,10.0,'FRAME',5,'AMP',3,Z,H,M,0.15,-6,Z,SIG,M,
     $0.15,-5,Z,XG,M,0.15,-3,Z,YG,M,0.15,-1,Z,YO,M,0.0,KS)
   15 CONTINUE
C
C     CALCULATE WAVELENGTH
C
      WRITE(6,16)
   16 FORMAT ('1')
      XLAM = G / (2 * PI * FREQ ** 2)
      XLAM1 = XLAM
   17 CORR = TANH((2 * PI * DEP) / XLAM)
      ERR = XLAM / CORR - XLAM1
      XLAM = XLAM - (0.7 * CORR * ERR)
      WRITE(6,18) XLAM
   18 FORMAT ('0XLAM = ',F9.5)
```

```
      IF (ABS(ERR) - 0.0001) 19, 19, 17
   19 CONTINUE
      WRITE(6,20) XLAM, XLAM1, ERR
   20 FORMAT ('0LAMDA = ',F9.5,'          LAMDA1 = ',F9.5,'          ER
     $R = ',E9.3)
C
C     CALCULATE NUMBER OF DATA POINTS IN 1 CYCLE
C
      CALL NPOINT (H,NI)
      NR = NI
      NP = 2 * NR + 1
      WRITE(6,21) NP
   21 FORMAT ('1NPOINT =',I4)
C
C     CALCULATE FIRST AND SECOND ORDER FOURIER COFFICIENTS
C
      WRITE(6,22)
   22 FORMAT ('0 ACOF(1)        ACOF(2)        ACOF(3)        BCOF(2)
     $     BCOF(3)')
      IT = 3
      CALL FORIER (H,NR,IT,ACOFH,BCOFH,NOP)
      CALL FORIER (XG,NR,IT,ACOFXG,BCOFXG,NOP)
      CALL FORIER (YG,NR,IT,ACOFYG,BCOFYG,NOP)
C
C     CALCULATE AND PRINT KA, MAGNITUDE X/A, PHASE X/A
C
      K = 2 * PI / XLAM
      KA = K * D
      X = SQRT(ACOFXG(2) ** 2 + BCOFXG(2) **2)
      HA = SQRT(ACOFH(2) ** 2 + BCOFH(2) ** 2)
      XDH = X / HA
      XGPHAS = ATAN2(BCOFXG(2), ACOFXG(2))
      HPHAS = ATAN2(BCOFH(2), ACOFH(2))
      PHASE = HPHAS + 2 * PI * XA / XLAM - XGPHAS
      WRITE(6,23)
   23 FORMAT ('1  KA        MAGNITUDE X/A     PHASE X/A      MAG X        M
```

```
  $AG A       PHASE X       PHASE A')
   WRITE(6,24) KA, XDH, PHASE, X, HA, XGPHAS, HPHAS
24 FORMAT ('0',F8.4,2F15.4,4F12.4)
25 CONTINUE
   IF (NOP) 26, 26, 27
26 CALL ENDPLT
27 CONTINUE
   STOP
   END
```

```
      SUBROUTINE FORIER (FN,NR,IT,ACOF,BCOF,NOP)
      DIMENSION HFOR1(300), HFOR2(300), ACOF(5), BCOF(5), Z(300),
     $YO(300), FN(300)
      PI = 3.14159
      NP = 2 * NR + 1
      NX = 0
      W = 2 * PI / NP
      CALL FORIT (FN,NR,IT,ACOF,BCOF,IER)
      IF (IER - 1) 3, 1, 1
    1 WRITE(6,2) IER
    2 FORMAT ('0IER = ',I1)
    3 WRITE(6,4) ACOF(1), ACOF(2), ACOF(3), BCOF(2), BCOF(3)
    4 FORMAT ('0',F8.5,4F15.5)
C
C     PLOT DATA WITH 1ST AND 1ST + 2ND FOURIER COMP. CURVES (OPTIONAL)
C
      IP = 1
      IF (IP - NOP) 7, 7, 5
    5 DO 6 I = 1, NP
      HFOR1(I) = ACOF(1) + ACOF(2) * COS(W * NX) + BCOF(2) * SIN(W * NX)
      HFOR2(I) = HFOR1(I) + ACOF(3) * COS(2 * W * NX) + BCOF(3) *
     $SIN(2 * W * NX)
      Z(I) = I
      YO(I) = 0
    6 NX = NX + 1
      CALL PICTUR (10.0,10.0,'FRAME',5,'AMP',3,Z,FN,NP,0.15,-3,Z,HFOR1,
     $NP,0.10,-2,Z,HFOR2,NP,0.10,-1,Z,YO,NP,0.0,KS)
    7 CONTINUE
      RETURN
      END
```

```
      SUBROUTINE NPOINT (H,NR)
      DIMENSION H(300)
      I = 2
      IF (H(1)) 8, 8, 1
    1 IF (H(I)) 3, 3, 2
    2 I = I + 1
      GO TO 1
    3 IA = I
    4 IF (H(I)) 5, 6, 6
    5 I = I + 1
      GO TO 4
    6 IF (H(I)) 15, 15, 7
    7 I = I + 1
      GO TO 6
    8 IF (H(I)) 9, 10, 10
    9 I = I + 1
      GO TO 8
   10 IA = I
   11 IF (H(I)) 13, 13, 12
   12 I = I + 1
      GO TO 11
   13 IF (H(I)) 14, 15, 15
   14 I = I + 1
      GO TO 13
   15 IB = I
      IC = IB - IA
      ID = IC / 2
      IE = 2 * ID
      IF (IC - IE) 16, 16, 23
   16 IG = IB + 1
      IF (H(IB) - H(IA)) 17, 17, 20
   17 IF (H(IG) - H(IB)) 18, 18, 19
   18 NP = IC - 1
      GO TO 24
   19 NP = IC + 1
      GO TO 24
```

```
20 IF (H(IG) - H(IB)) 21, 21, 22
21 NP = IC + 1
   GO TO 24
22 NP = IC - 1
   GO TO 24
23 NP = IC
24 NR = (NP - 1) / 2
   RETURN
   END
```

APPENDIX B

The theoretical values for the magnitude and phase of /A were computed as a function of Ka using a Fortran program. From Eq. 53, the relation for the magnitude is given by

$$\frac{\chi}{A} = \frac{S}{(Q^2 + R^2)^{1/2}} \tag{B-1}$$

where Q, R, and S are as defined in Eq. 52, 53, and 51. Also from Eq. 55 the phase angle, ζ is seen to be

$$S = \theta + \tan^{-1}(-R/Q) \tag{B-2}$$

where θ is defined by Eq. 44.

A listing of the actual program used follows in which these symbols were used

AD	boom draft
AMASS	added mass of fluid
BL	boom length
BM	boom mass
CHI	magnitude of χ/A
DEP	water depth
PHASE	phase of χ/A
TN	tension force
XKA	Ka
XL	length of tension members

YPD P_d, drag coefficient

YPH $\tan^{-1}$ (G/-H)

YPM P_M, added mass coefficient

```
      DIMENSION XKA(50), YPD(50), YPM(50), YPH(50), XKA1(50), XKA2(50),
     $XKA3(50), XKA4(50), CHI1(50), CHI2(50), CHI3(50), CHI4(50),
     $PHASE1(50), PHASE2(50), PHASE3(50), PHASE4(50), X(50), Y(50),
     $Z(50)
C
C     READ IN VALUES OF PD, PM, ARCTAN(G/-H)
C
      DO 2 I = 1, 29
      READ (5,1) XKA(I), YPD(I), YPM(I), YPH(I)
    1 FORMAT (4F10.4)
    2 CONTINUE
      READ (5,3) T1, T2, T3, T4
    3 FORMAT (4F10.2)
      WRITE (6,6) T1
      WRITE (6,7)
C
C     CALL SUBROUTINE TO CALCULATE MAGNITUDE AND PHASE OF X/A
C
      CALL CALC(T1,XKA,XKA1,YPD,YPM,YPH,CHI1,PHASE1)
      WRITE (6,6) T2
      WRITE (6,7)
      CALL CALC(T2,XKA,XKA2,YPD,YPM,YPH,CHI2,PHASE2)
      WRITE (6,6) T3
      WRITE (6,7)
      CALL CALC(T3,XKA,XKA3,YPD,YPM,YPH,CHI3,PHASE3)
      WRITE (6,6) T4
      WRITE (6,7)
      CALL CALC(T4,XKA,XKA4,YPD,YPM,YPH,CHI4,PHASE4)
      DO 5 I = 1, 22
      READ (5,4) X(I), Y(I), Z(I)
    4 FORMAT(3F10.2)
    5 CONTINUE
C
C     PLOT DATA
C
      CALL NEWPLT ('M7754','8427','WHITE ','BLACK')
```

```
      CALL PICTUR(15.5,10.0,'KA',2,'MAGNITUDE X/A',13,X,Y,22,0.2,-4,XKA1
     $,CHI1,29,0.0,J,XKA2,CHI2,29,0.0,J,XKA3,CHI3,29,0.0,J,XKA4,CHI4,
     $29,0.0,J)
      CALL PICTUR(15.5,10.0,'KA',2,'PHASE X/A',9,X,Z,22,0.2,-4,XKA1,PHAS
     $E1,29,0.0,J,XKA2,PHASE2,29,0.0,J,XKA3,PHASE3,29,0.0,J,XKA4,PHASE4,
     $29,0.0,J)
      CALL ENDPLT
    6 FORMAT ('1T = ',F10.2)
    7 FORMAT ('0  KA    MAG X/A      PHASE    LAMDA       OMEGA            Q
     $               R                S       ZETA    THETA')
      STOP
      END
```

```
      SUBROUTINE CALC(T,XKA,XKAN,YPD,YPM,YPH,CHI,PHASE)
      DIMENSION XKA(50), XKAN(50), YPD(50), YPM(50), YPH(50), CHI(50),
     $PHASE(50)
C
C     INITIAL SETUP
C
      RHO = 1.0
      G = 980.35
      BL = 30.0
      BMASS = 39.8
      PI = 3.14159
      AD = 2.4
      DEP = 15.0
      XL = 50.0
      AMASS = RHO * PI * AD ** 2 * BL / 2
C
C     CALCULATE VALUES FOR MAGNITUDE AND PHASE OF X/A
C
      DO 2 I = 1, 29
      XKAN(I) = XKA(I)
      S = RHO * G * AD* BL * SQRT(PI * YPD(I) / 2)
      XLAM = 2 * PI * AD / XKA(I)
      OMEGA = SQRT(((G * 2 * PI) / XLAM) * TANH((2 * PI * DEP) / XLAM))
      Q = ((BMASS + YPM(I) * AMASS) * OMEGA ** 2) - (2 * T / XL)
      R = - (YPD(I) * AMASS * OMEGA ** 2)
      CHI(I) = S / SQRT(Q ** 2 + R ** 2)
      ZETA = ATAN(- R / Q)
      THETA = (PI /  2) - YPH(I)
      PHASE(I) = THETA + ZETA - PI
      WRITE (6,1) XKA(I), CHI(I), PHASE(I), XLAM, OMEGA, Q, R, S, ZETA,
     $THETA
    1 FORMAT ('0',F5.2,4F10.4,3F15.4,2F8.4)
    2 CONTINUE
      RETURN
      END
```

REFERENCES

1. F. Ursell, "On the Waves Due to the Rolling of a Ship," Quarterly Journal of Mechanics and Applied Mathematics, Vol. 1, 1948, pp. 246-252.

2. G. H. Watson, Theory of Bessel Functions, University Press, second edition, 1952, pp. 77, 78, 329.

3. J. Kotik, "Damping and Inertia Coefficients for a Rolling or Swaying Vertical Strip," Journal of Ship Research, Vol. 7, No. 2, October 1963, pp. 19-23.

4. M. D. Haskind, "The Exciting Forces and Wetting of Ships in Waves," Izvestia Akademii Nauk S.S.S.R., Otdelenie Teckhnicheskikh Nauk, No. 7, 1957, pp. 65-79. (English translation available as David Taylor Model Basin Translation No. 307, March 1962).

5. J. N. Newman, "The Exciting Forces on Fixed Bodies in Wave," Journal of Ship Research, Vol. 6, December 1962, pp. 10-17.

6. G. H. Keulegan and Lloyd H. Carpenter, "Forces on Cylinders and Plates in an Oscillating Fluid," Journal of Research of the National Bureau of Standards, Vol. 60, No. 5, May, 1958, pp. 423-440.

Ka	P_D	P_M	$-\tan^{-1}(G/-H)$
0.05	0.0043	1.0436	0.0050
0.1	0.0176	1.1041	0.0160
0.15	0.0423	1.1710	0.0345
0.2	0.0808	1.2334	0.0660
0.25	0.1350	1.2980	0.1075
0.3	0.2133	1.3690	0.1547
0.4	0.4302	1.4706	0.2854
0.5	0.7244	1.4750	0.4549
0.6	0.0046	1.3361	0.6476
0.7	1.1934	1.0837	0.8385
0.8	1.2505	0.8063	1.0060
0.9	1.2095	0.5722	1.1407
1.0	1.1211	0.4012	1.2439
1.1	1.028	0.2940	1.3216
1.2	0.940	0.2079	1.3796
1.3	0.852	0.1580	1.4232
1.4	0.778	0.1260	1.4560
1.5	0.707	0.1058	1.4811
1.6	0.641	0.0936	1.5003
1.7	0.585	0.0870	1.5151
1.8	0.534	0.0835	1.5267
1.9	0.489	0.0826	1.5357
2.0	0.451	0.0839	1.5428
2.5	0.330	0.1026	1.5615
3.0	0.245	0.1279	1.5676
3.5	0.195	0.1527	1.5684
4.0	0.158	0.1758	1.5692
4.5	0.127	0.1950	1.5700
5.0	0.099	0.2142	1.5707

Table 1: Values of P_D, P_M, and $-\tan^{-1}(G/-H)$ for Ka = 0.05 through 5.0.

Ka	Magnitude of χ/A	Phase of χ/A	Q	R	S
0.05	0.725	-1.577	-8003.6	-7.2	5801.1
0.10	5.077	-1.634	-2309.2	-108.2	11736.2
0.15	2.979	-1.521	-6086.2	-516.4	18194.6
0.20	1.569	-1.542	15959.2	-1519.9	25146.6
0.25	1.209	-1.551	26672.5	-3427.0	32504.2
0.30	1.056	-1.550	38096.7	-6768.8	40857.2
0.40	0.912	-1.556	60763.7	-18823.9	58024.0
0.50	0.846	-1.560	79552.3	-40004.0	75294.2
0.60	0.800	-1.572	88529.1	-66756.8	88668.4
0.70	0.767	-1.584	85457.8	-92592.7	96641.9
0.80	0.740	-1.598	74516.8	-110908.7	98926.9
0.90	0.718	-1.614	61727.9	-120689.1	97291.6
1.00	0.700	-1.632	50739.8	-124300.4	93668.8
1.10	0.678	-1.657	43739.8	-125376.4	89695.2
1.20	0.657	-1.669	37169.8	-125066.2	85770.2
1.30	0.641	-1.693	33908.3	-122804.5	81656.8
1.40	0.624	-1.717	32318.7	-120764.4	78030.1
1.50	0.610	-1.747	31981.9	-117582.4	74384.4
1.60	0.599	-1.780	32616.4	-113712.8	70827.4
1.70	0.586	-1.815	34036.0	-110264.6	67662.3
1.80	0.575	-1.852	35927.8	-106572.6	64646.3
1.90	0.563	-1.892	38289.8	-103013.6	61862.5
2.00	0.549	-1.933	41119.7	-100008.8	59410.2
2.50	0.467	-2.135	59082.9	-91471.5	50819.4
3.00	0.380	-2.352	81314.9	-81492.8	43788.1
3.50	0.300	-2.520	106158.0	-75671.9	39065.2
4.00	0.234	-2.655	132996.8	-70072.7	35164.3
4.50	0.183	-2.765	160451.0	-63364.8	31526.4
5.00	0.141	-2.860	190033.9	-54882.9	27834.9

Table 2 Theoretical values for magnitude and phase of /A along with values for Q, R, and S for Ka = 0.05 through 2.0 with τ = 0.142.

Run	Ka	Magnitude X/A	Phase X/A
A2	0.142	3.169	-1.329
A6	0.139	2.172	1.365
A10	0.144	1.885	-1.318
B2	0.202	1.770	-1.772
B6	0.202	1.425	-1.547
C2	0.291	0.963	-1.731
C5	0.299	1.027	-1.419
C8	0.300	0.910	-1.497
D2	0.467	0.836	-1.605
D3	0.536	0.775	-1.582
D4	0.536	1.043	-1.284
E1	0.784	0.808	-1.433
E2	0.767	0.646	-1.461
F1	1.376	0.824	-1.004
G2	0.391	1.042	-1.349
G4	0.388	1.015	1.395

Table 3: Experimental values of magnitude and phase of X/A along with values of wavelength and wave height.

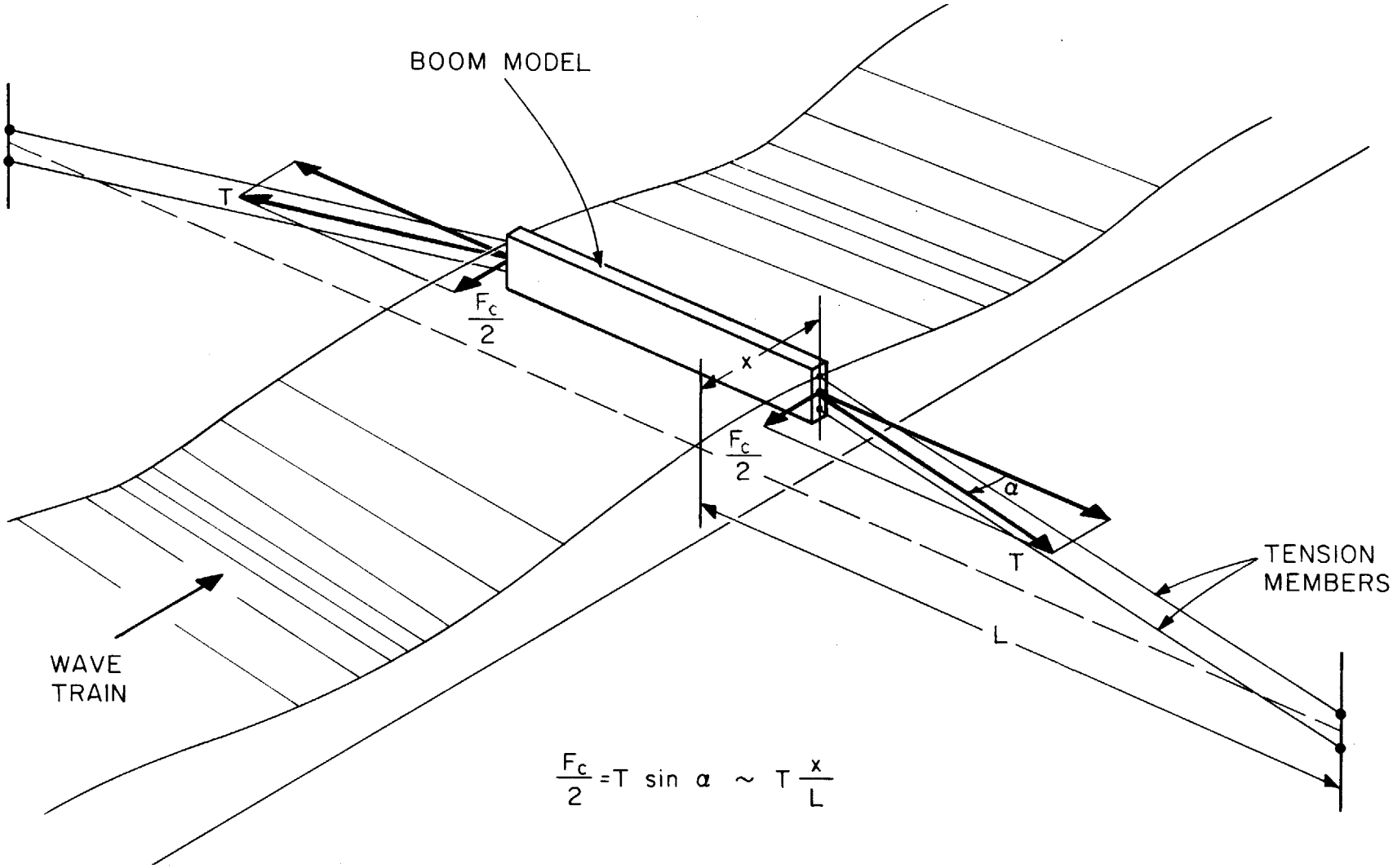

Fig. 1 Schematic of constraint forces on model boom.

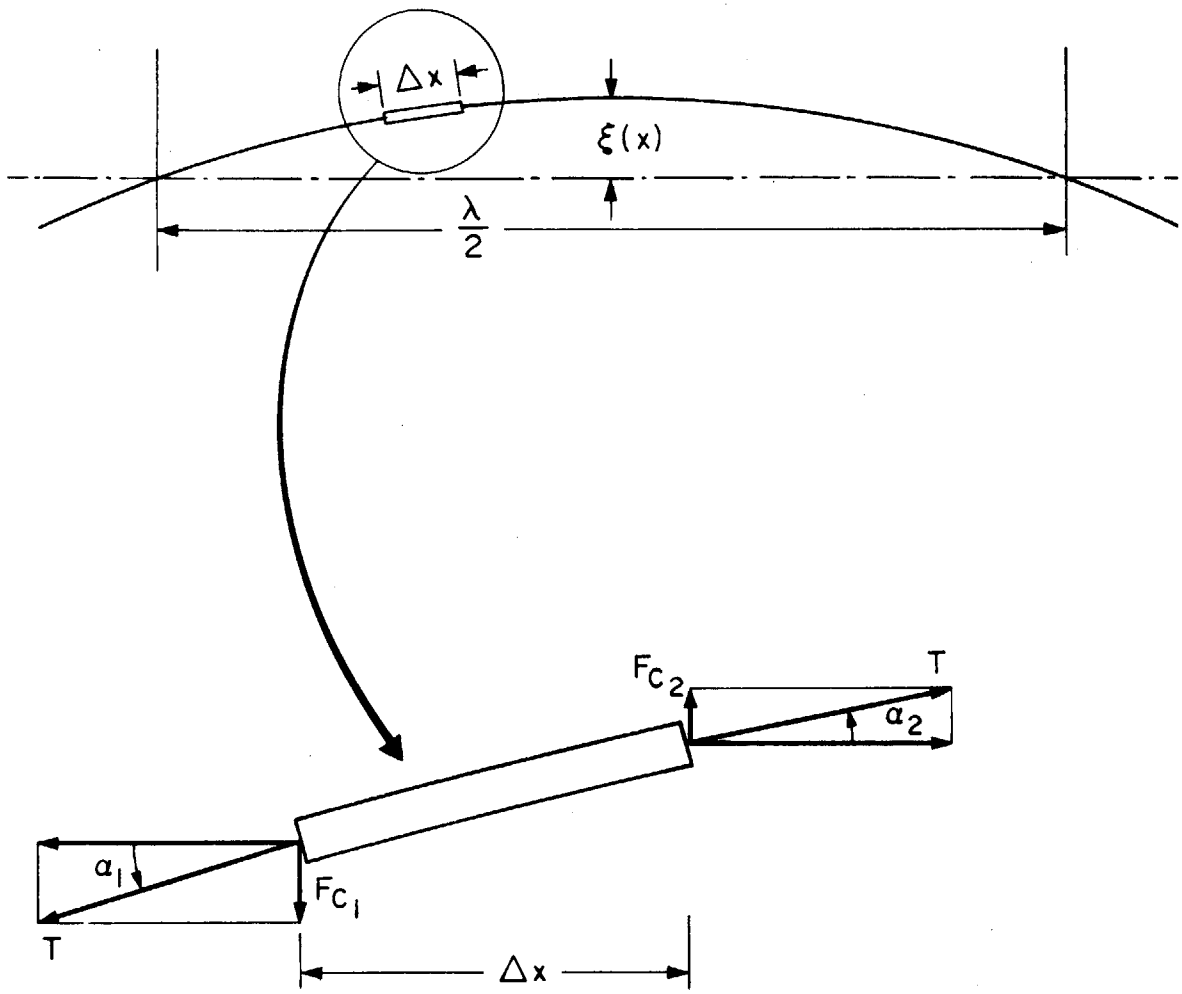

$$F_{C_n} = T \sin \alpha_n = T \left.\frac{\partial \xi}{\partial x}\right|_n$$

$$F_C = \frac{T\left(\left.\frac{\partial \xi}{\partial x}\right|_2 - \left.\frac{\partial \xi}{\partial x}\right|_1\right)}{\Delta x}$$

Fig. 2 Schematic of constraint forces on full scale boom.

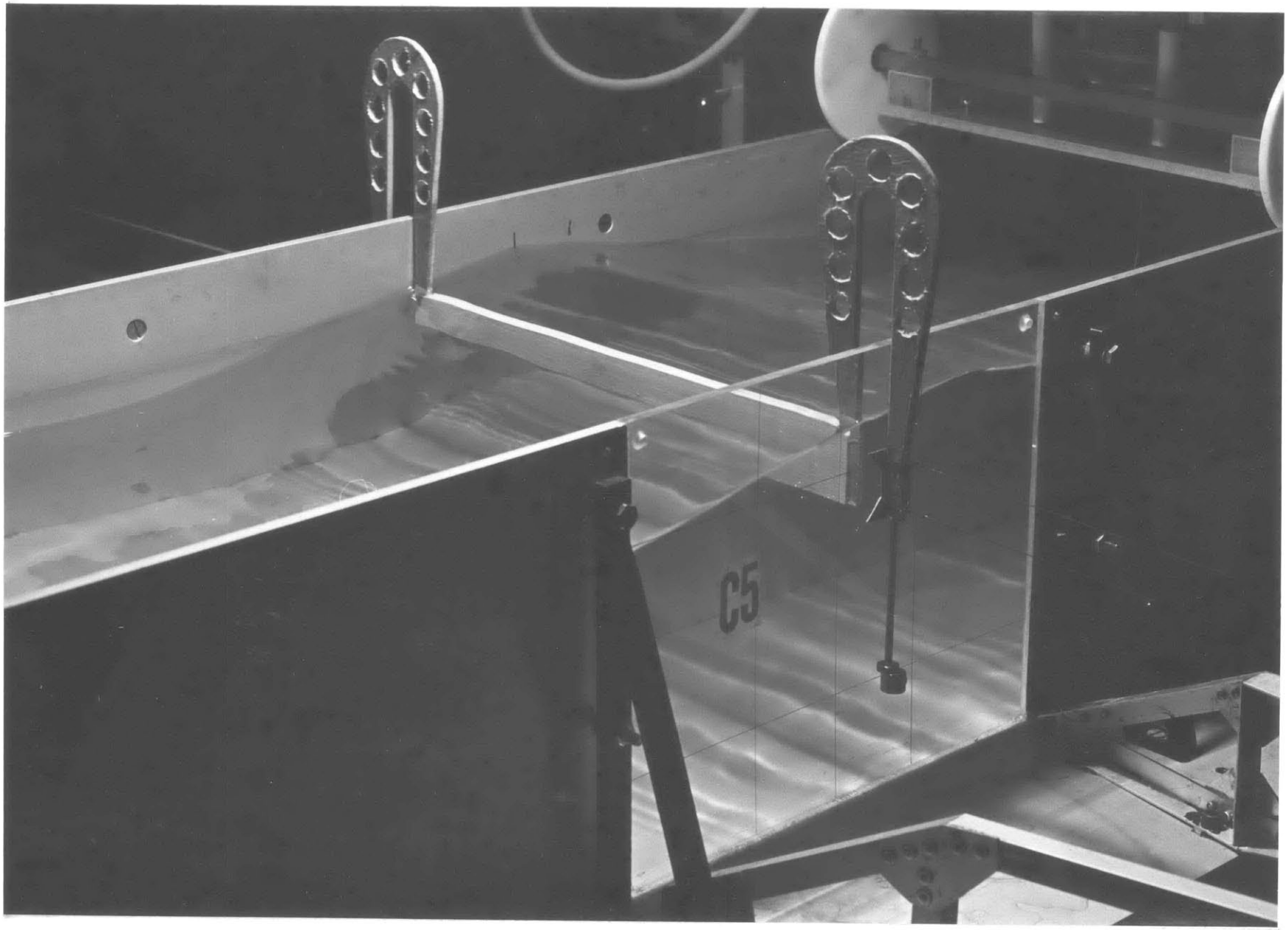

Fig. 3 Close-up photograph of boom in wave tank during experimental run C5 (Ka = 0.30).

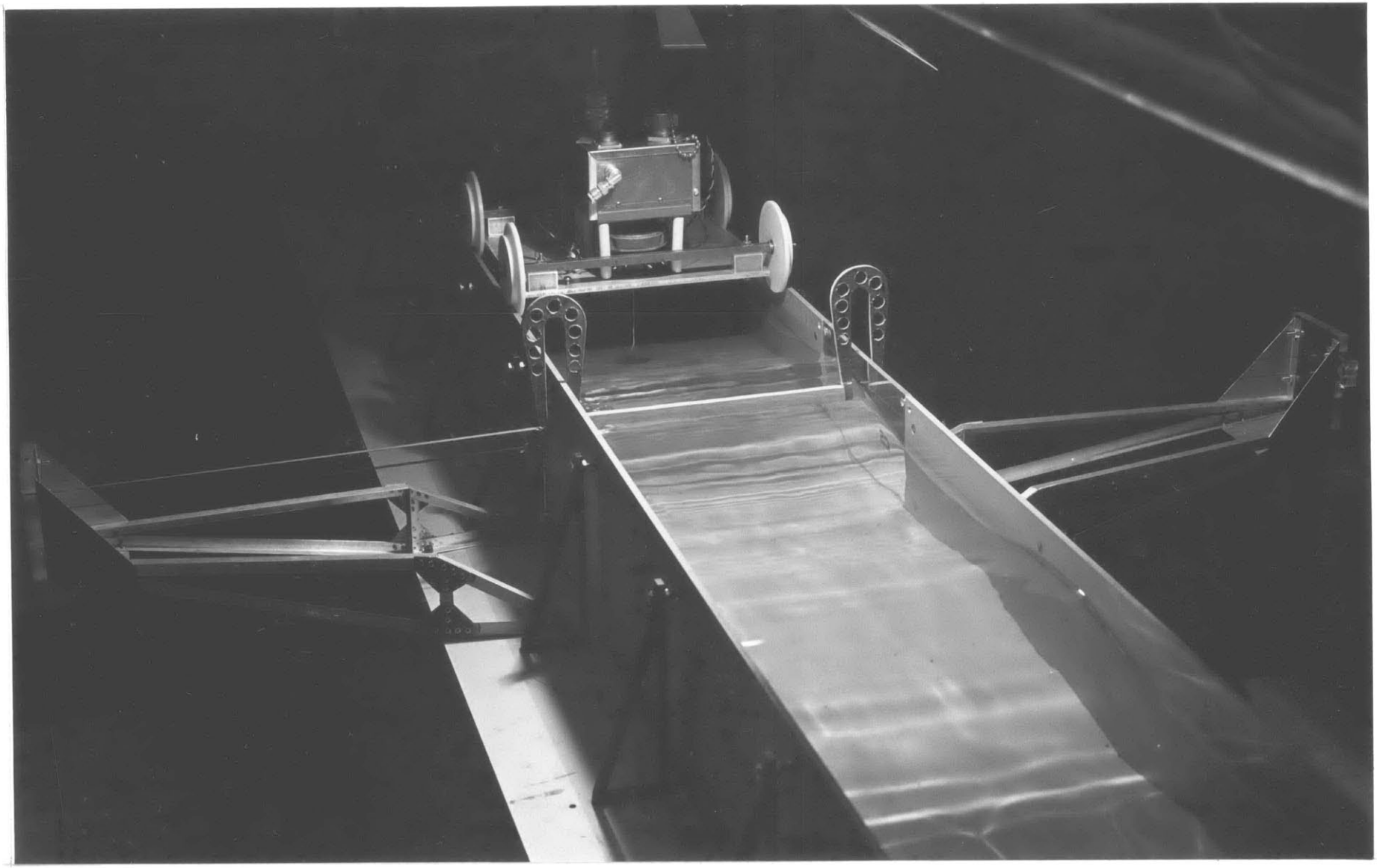

Fig. 4 Overall view of boom in wave tank showing elastic constraint support arms and capacitance wave height guage (on carriage behind the boom model).

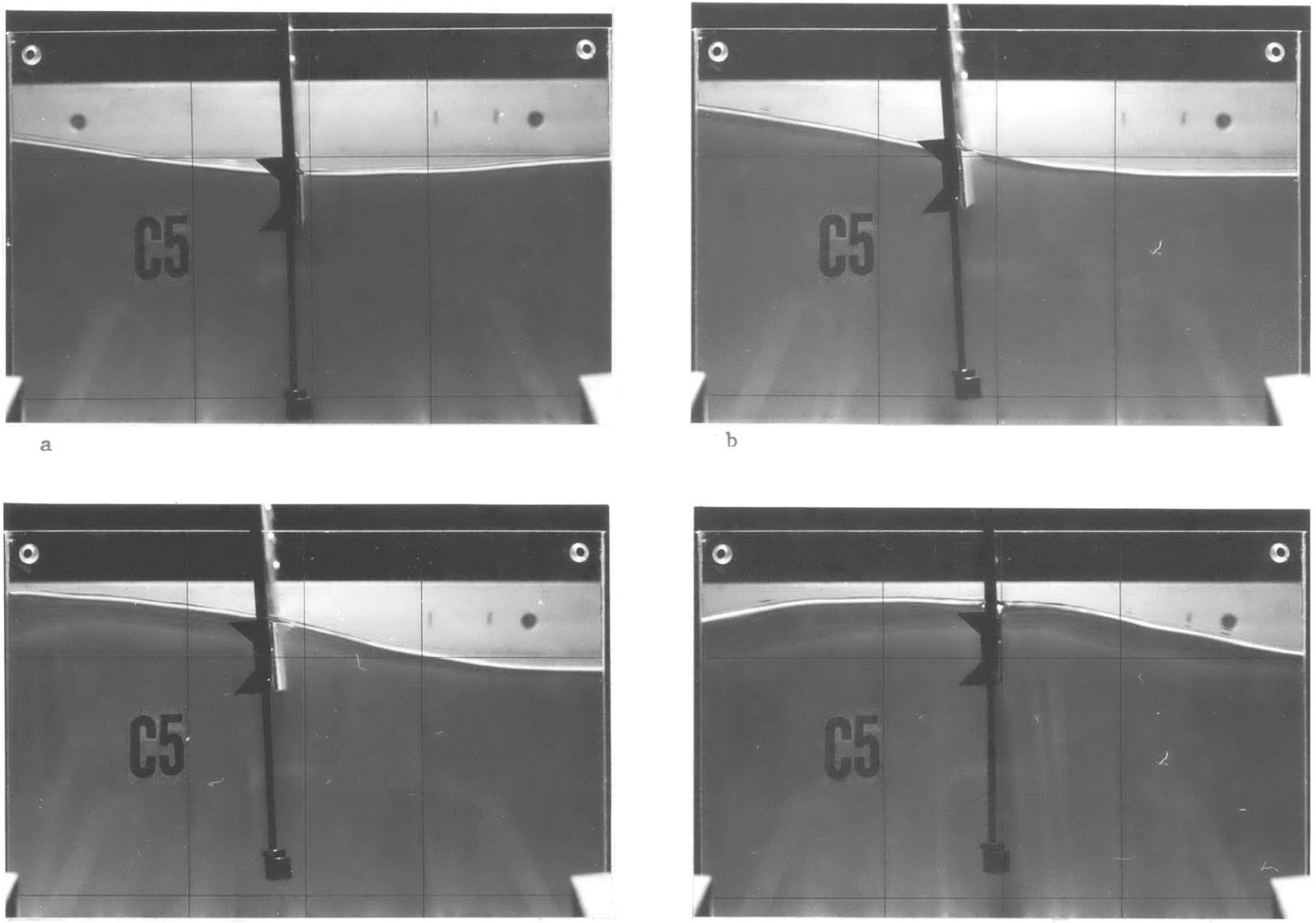

a b

c d

Fig. 5 Sequence of boom positions during experimental run C5 (Ka = 0.30). Photographs were taken with a motor-driven 35 mm still camera showing the same view as the data films.

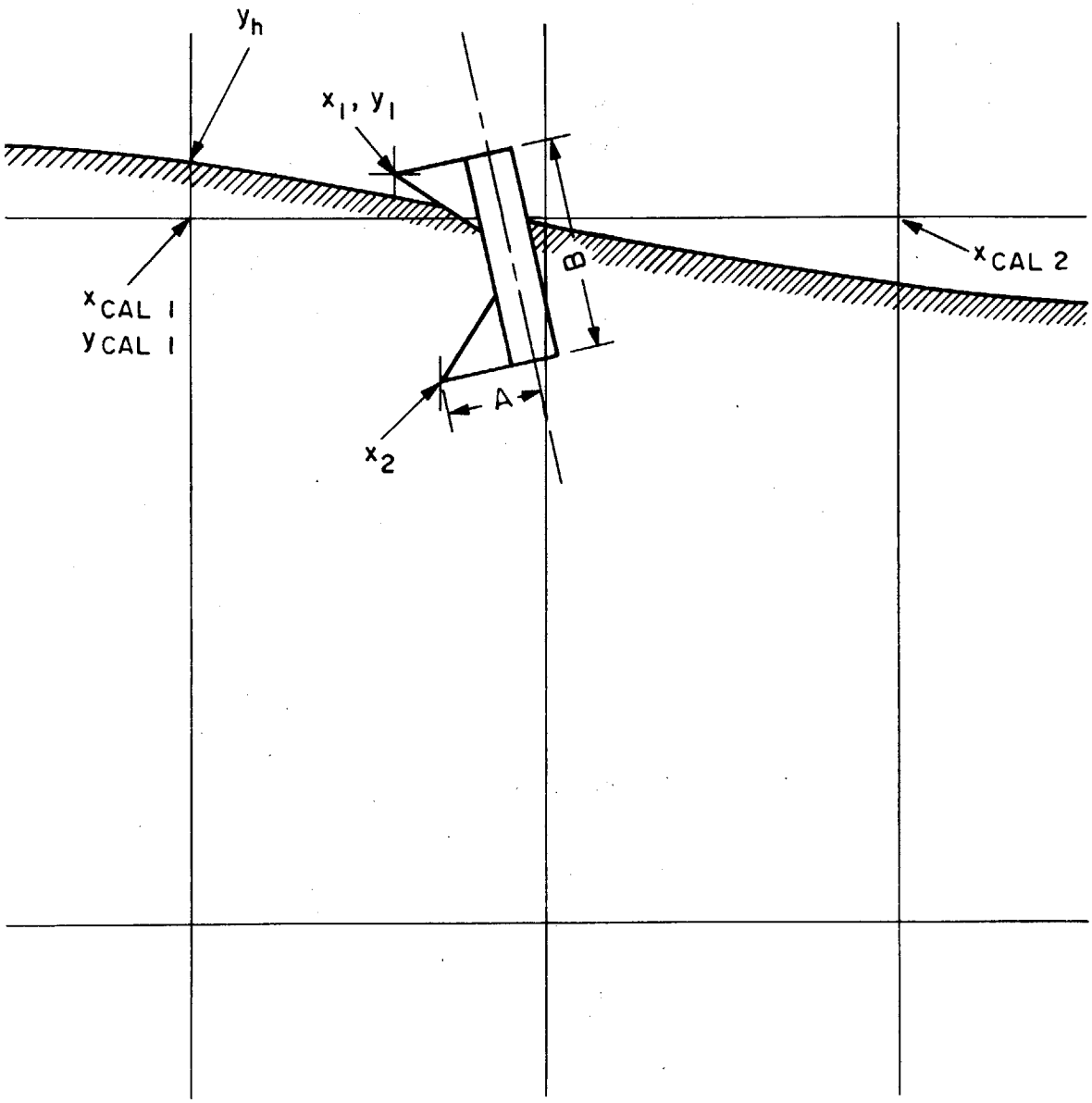

Fig. 6 Drawing of measurement grid lines and boom pointer illustrating measurement points.

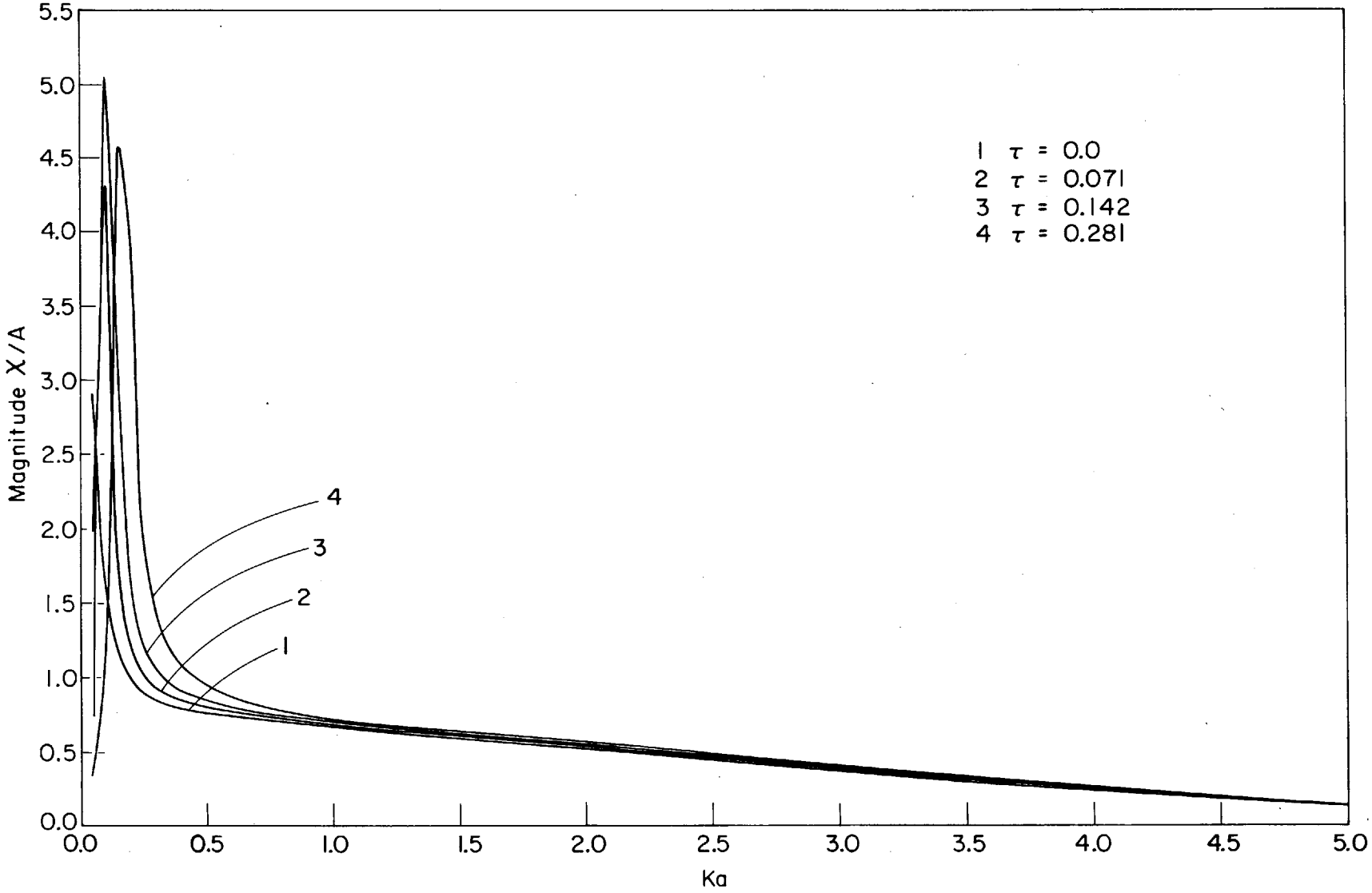

Fig. 7 Plot of the theoretical values of the magnitude of χ/A for Ka = 0.05 through 5.0 with τ = 0, 0.071, 0.142, 0.281.

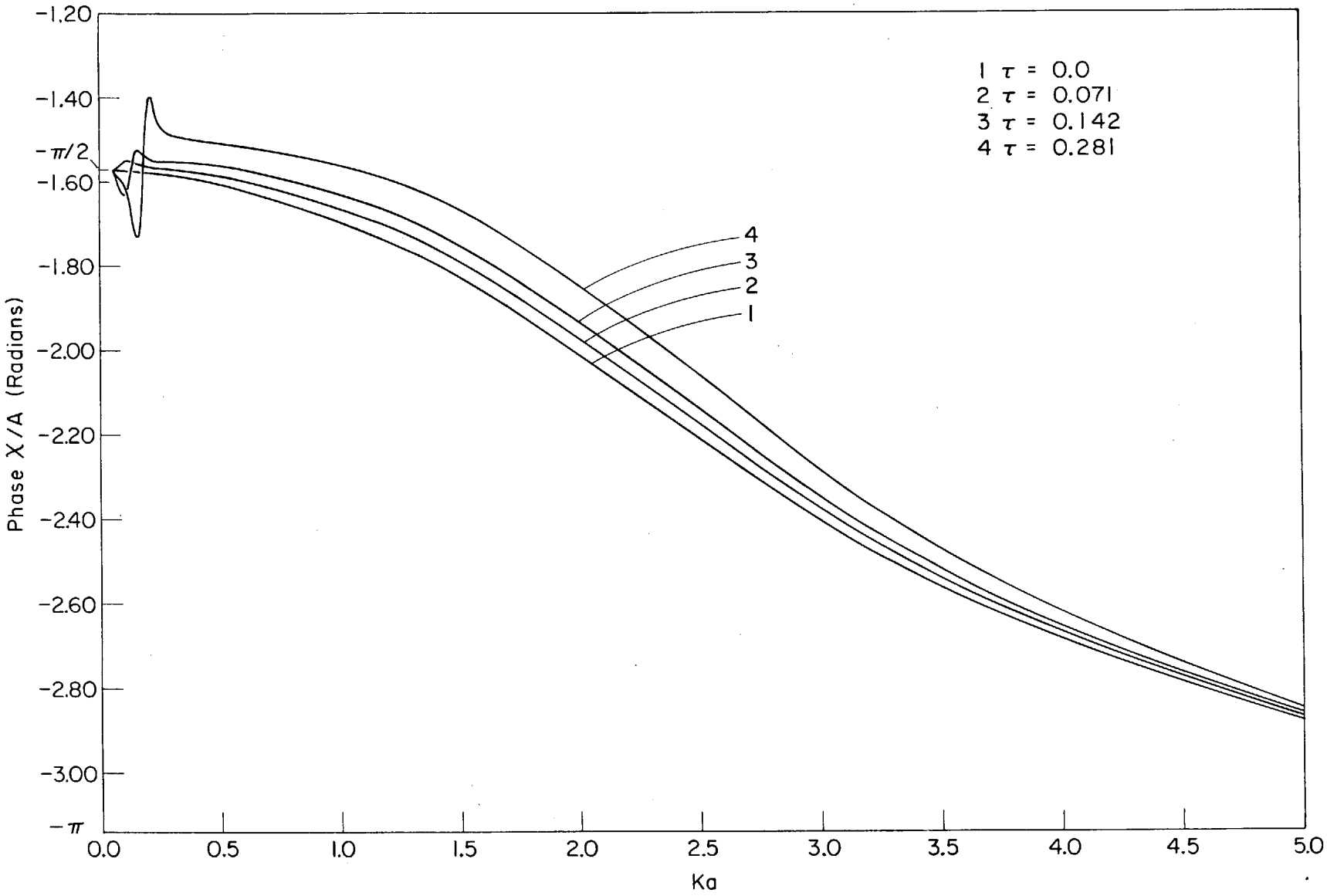

Fig. 8 Plot of the theoretical values for the phase of χ/A for Ka = 0.05 through 5.0 with τ = 0, 0.071, 0.142, 0.281.

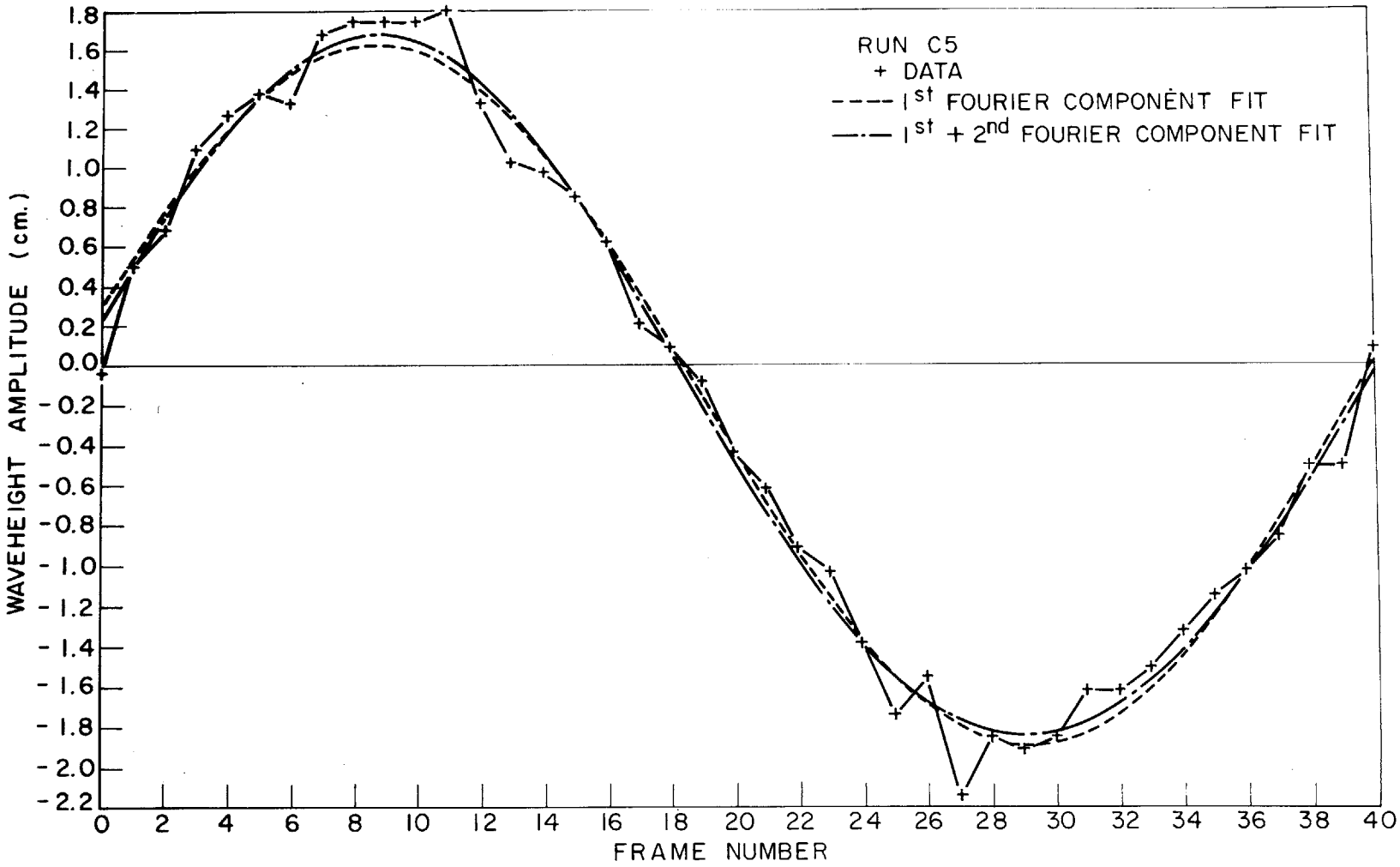

Fig. 9 Example of wave height data from run C5 with curves using the first fourier coefficients and the first and second fourier coefficients.

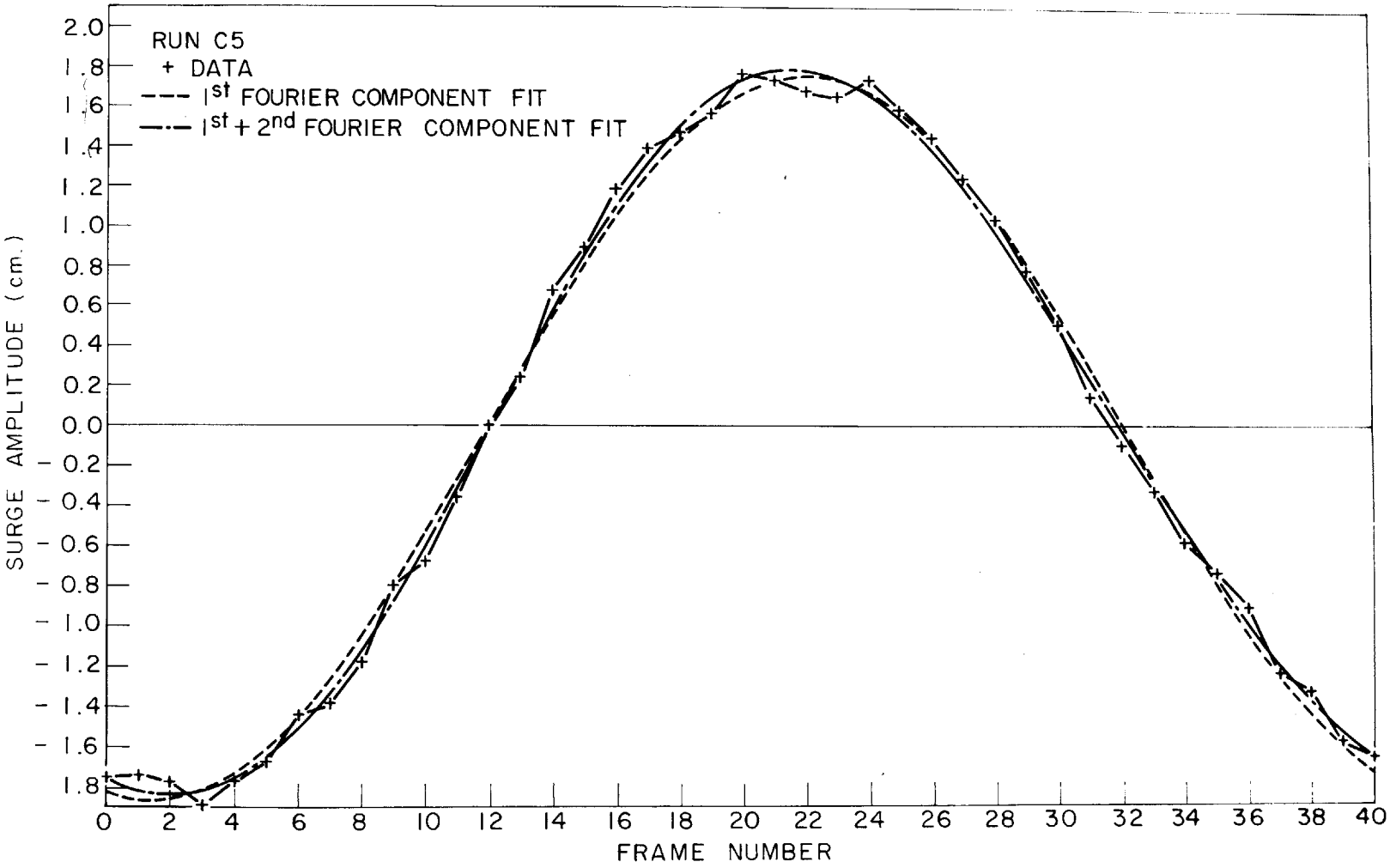

Fig. 10 Example of surge displacement data from run C5 with curves using the first fourier coefficients and the first and second fourier coefficients.

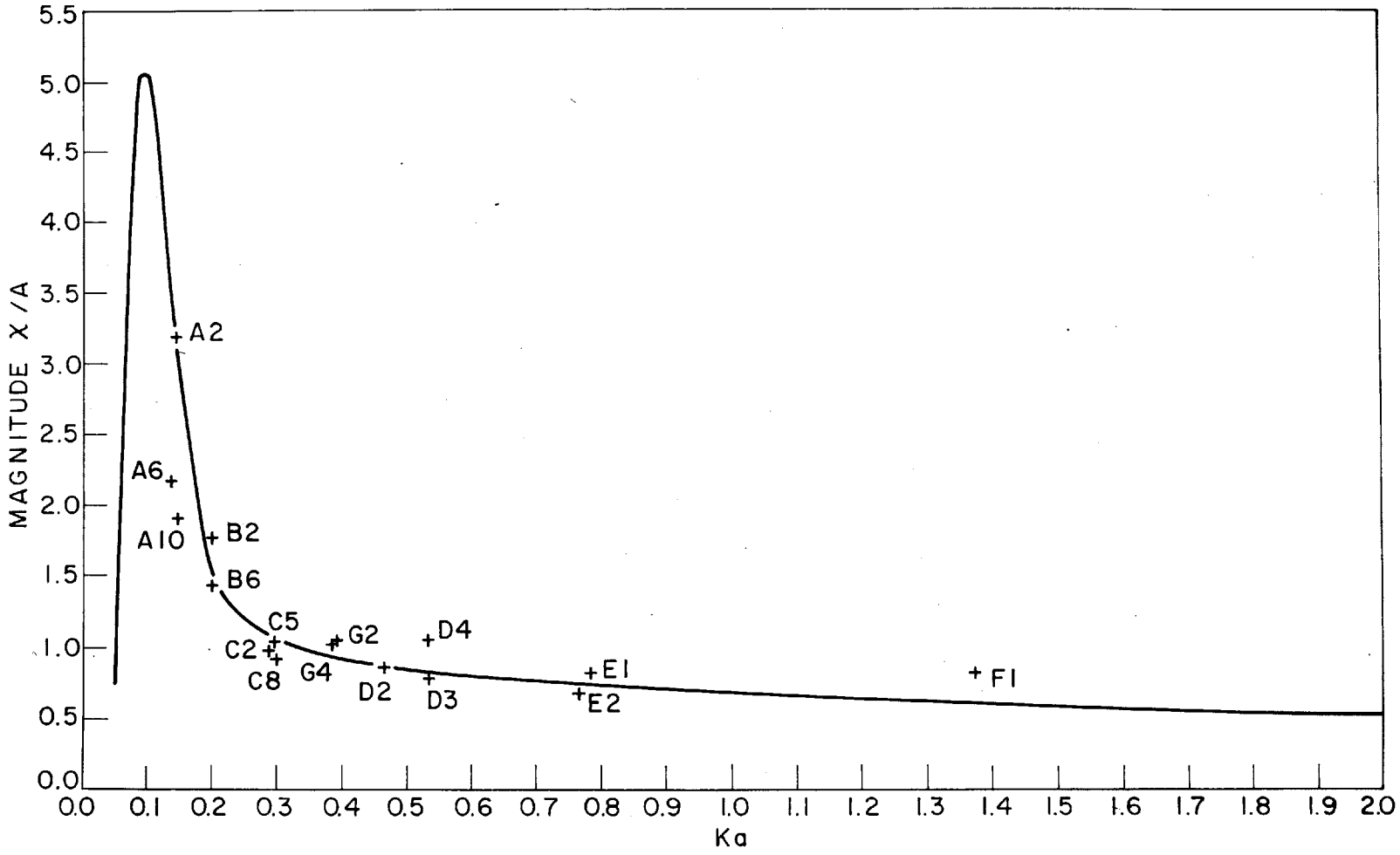

Fig. 11 Plot of the theoretical values of the magnitude of χ/A with the experimental data points for Ka = 0.05 thru 2.0 and τ = 0.142.

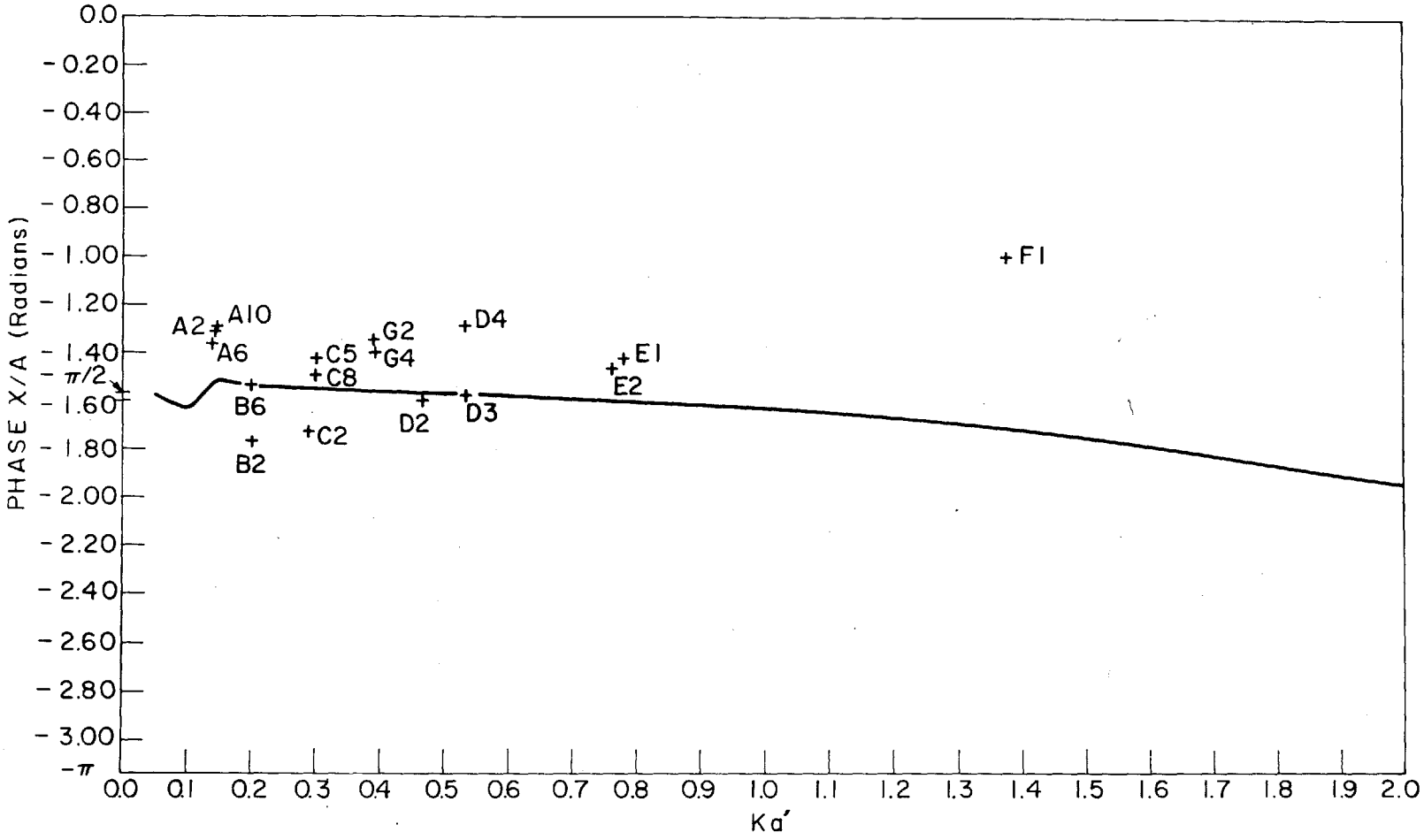

Fig. 12 Plot of the theoretical values of the phase of χ/A with the experimental data points obtained for Ka = 0.05 thru 2.0 and τ = 0.142.